NCGIA

National Center for Geographic Information and Analysis

The Use of Vegetation Maps and Geographic Information Systems For Assessing Conifer Lands in California

By

Michael F. Goodchild, Frank W. Davis,
Marco Painho, and David M. Storns

University of California, Santa Barbara

Technical Report 91-23
August 1991

Simonett Center for Spatial Analysis
University of California
35 10 Phelps Hall
Santa Barbara, CA 93106-4060
Office (805) 893-8224
Fax (805) 893-8617
ncgia@ncgia.ucsb.edu

State University of New York
301 Wilkeson Quad, Box 610023
Buffalo NY 14261-0001
Office (716) 645-2545
Fax (716) 645-5957
ncgia@ubvms.cc.buffalo.edu

University of Maine
348 Boardman Hall
Orono ME 04469-5711
Office (207) 581-2149
Fax (207) 581-2206
ncgia@spatial.maine.edu

Table of Contents

PROJECT SUMMARY

This report summarizes research into the nature and sources of errors that occur in medium to small scale vegetation maps such as those used for statewide forestry and conservation planning. The objective of this research was to develop a coherent approach and specific methods for quantifying such errors by jointly analyzing ground observations and multiscale map data using Geographic Information Systems (GIS) operations.

Section I of the report provides an overview of statistical approaches to assessing cartographic errors, including uncertainty in points, lines, irregular polygons and classified digital imagery. Techniques for assessing point errors and line digitizing errors are relatively well developed. By comparison, much research is still needed on methods for comparing polygon and image data to ground measurements. Another active research front deals with propagation of errors during GIS analyses involving multiple spatial data layers. Also, work is needed to find effective means of transmitting accuracy information to the user of spatial data.

Section 2 describes an error analysis of the CALVEG map of vegetation in California. The purpose of the analysis was to demonstrate a variety of approaches to assessing map accuracy, rather than to provide a formal test of the CALVEG map. The map is compared to ground data, U.S. Forest Service photo plots and larger scale timber inventory maps using GIS operations of overlay and spatial analysis. Analyses proceed from contingency table comparisons to analyses of spatial properties of map errors, including spatial autocorrelation, boundary effects, map generalization and association of errors with environmental variables. The tests and their results are summarized in a table at the end of this section. In general, high error rates were documented for the CALVEG map, and these errors were shown to have a number of different sources, most importantly polygon misclassification and map generalization.

The report concludes with a series of recommendations to CDF concerning changes in map accuracy assessment procedures. These recommendations pertain to data collection, sampling design, and methods for representing uncertainty in map products. Specific recommendations include the use of enhanced mapping procedures and measures of line quality, withinpolygon heterogeneity and within polygon vegetation texture.

Summary of Procedures and Results from an Error Analysis of the CALVEG Map

Error Type	Method of Assessment	Test Region	Result
NON-SPATIAL			
Classification Accuracy	Contingency table comparison to 78 randomly located field plots	Transverse Ranges and southern Sierra Nevada	31% Agreement, even after simplifying the vegetation classification.
	Contingency table comparison of CALVEG to 1347 FIA ground plots.	Statewide for forested regions	Overall agreement 30%, but varies widely among classes. Much of the confusion was between ecologically similar types, revealed by cluster analysis of the contingency matrix. Aggregation of non-conifer types increases map accuracy to 39%, with bias towards high producer accuracy (57%) and low consumer accuracy (33%). Map accuracy increases to 65% following simplification of the vegetation classification into 4 Formation types.
SPATIAL			
Regional differences in map accuracy	Contingency table analysis of FIA field data by region	Regions 1 through 5	Accuracy varies widely between regions from 18% in northeast California to 36% along the north coast.
Spatial relations of frequently confused types	Proximity analysis	Statewide for forested regions	Tested whether frequently confused conifer types tended to occur in adjacent polygons. There was mixed support for this hypothesis.
Autocorrelation of map errors	Variogram analysis of 1347 FIA ground plots coded correct/incorrect.	Statewide for forested areas	Errors exhibit local clustering to distances of 3-5 km, as well as large scale regional trends in error rates.
Boundary errors	Analyzed the distribution of FIA plot classification errors as a function of distance to the nearest polygon boundary	Statewide for forested areas	Error rates for most conifer types were higher near polygon boundaries, significantly so for the Redwood/Douglas Fir type.
Polygon digitizing errors	Digitizing trials by two analysts compared to CDF digital CALVEG map in terms of line displacement distances	Bakersfield test area	Displacement distances for the 2 analysts were normally distributed with 90% of the offsets less than 0.42 mm on the map (ground distance of 108 m). Offsets were much larger between maps produced at UCSB and the CDF map, with 90% of offsets less than 1.00 mm (ground distance of 252 m).

Map generalization errors	comparison of CALVEG polygons to photointerpreted transects and larger scale timber inventory maps	Bakersfield test area	Much fine scale variation in vegetation occurs within CALVEG polygons, but errors include polygon mislabeling as well as overgeneralization of vegetation heterogeneity
Relationship of map accuracy to environmental variables	Logit regression analysis of 1347 FIA ground plots	Statewide and by region	Classification errors were not significantly related to any of the environmental variables.

INTRODUCTION

Geographic Information Systems (GIS) make it possible to utilize different sets of spatial data and combine them to produce statistical as well as graphical reports (Tosta and Marose 1987). GIS output is often used in a planning and decision making framework, where any inaccuracy and bias of the output must be quantified and well understood. Unfortunately, there are many sources of inaccuracy in GIS data and methods for measuring and modeling the errors in GIS inputs and outputs are still developing (Goodchild 1989). Most geographic literature on the subject has only addressed individual aspects of cartographic error, such as the uncertainty of boundary location (e.g., Blakemore 1984; Mark and Csillag 1989) or attribute accuracy (e.g., Congalton 1988). In fact, accuracies in geometry and of attributes are often treated as independent factors.

We have investigated the kinds and sources of error that affect medium to small scale vegetation maps developed from remotely sensed data. Our objective has been to develop a more comprehensive approach to the measurement and modeling of map accuracy that includes analysis of attribute (classification) accuracy, boundary accuracy, spatial properties of map errors and the relationship of those errors to other mapped variables. This information is needed for vegetation maps to be objectively applied to regional and statewide vegetation inventories.

Section I of this report provides an overview of methods for determining the accuracy of thematic maps. In Section 2 we demonstrate some of these techniques in an accuracy assessment of conifer classes in the CALVEG map of the vegetation of California. We document the types of errors that occur in the production of digital vegetation maps, including non-random classification errors, boundary errors, errors introduced during digitizing and geometric rectification. Geographic Information System (GIS) operations such as map overlay, buffering, area and distance calculations are used to compare the CALVEG map to more detailed map and field survey data. Section 3 provides a summary of the research and recommends a strategy for assessing the accuracy of vegetation maps derived from remotely sensed data.

1. REVIEW OF STATISTICAL APPROACHES TO ASSESSING CARTOGRAPHIC ERROR

1.1. Introduction

Digital processing of cartographic data brings immense benefits in the form of rapid, precise and sophisticated analysis, but at the same time it reveals weaknesses that may not otherwise be apparent. Computers are very precise machines, and errors and uncertainties in data can lead to serious problems, not only in the form of inaccurate results but in the consequences of decisions made on the basis of poor data, and increasingly in legal actions brought by affected parties. The widespread use of digital technology, particularly GIS, to analyze map information has led to significant problems, and many of these are apparent in using GIS to assess conifer lands.

In this section we first review the dimensions of the accuracy problem, and discuss the premises and assumptions on which the remainder of the section is based. The second part reviews the models which are available for analyzing and understanding errors in spatial data. The section concludes with a summary of the current state of the art as it relates to estimation of forest resources.

The terms accuracy, precision, resolution and scale are used almost interchangeably in reference to spatial data, but we will need to establish more exact definitions for the purposes of this discussion. Accuracy refers to the relationship between a measurement and the reality which it purports to represent. Precision refers to the degree of detail in the reporting of a measurement or in the manipulation of a measurement in arithmetic calculations. Finally, the resolution of a data set defines the smallest object or feature which is included or discernible in the data. Scale and resolution are intimately related because there is a lower limit to the size of an object that can be usefully shown on a paper map. This limit is often assumed to be 0.5mm as a rule of thumb, so the effective resolution of a 1:1,000 map is about 1,000 times 0.5mm, or 50cm, although the standards of most mapping agencies are substantially better. The effective resolutions of some common map scales, assuming 0.5mm resolution, are shown in Table 1.

Because digital spatial data sets are not maps, and have no similar physical existence, they do not have an obvious scale, and it is common to think of such data as essentially scalefree. But this is an oversimplification. If the data were obtained by digitizing, their resolution is that of the digitized map. If they were obtained from imagery, their resolution is that of the pixel size of the imagery. In spite of appearances to the contrary, then, no spatial data is ever resolution free. The term 'scale' is often used loosely as a surrogate for database resolution.

Table 1. Scale and resolution for some common map scales.

Scale	Effective Resolution (meters)	Minimum Area (hectares)
1:1,000	0.5	0.000025
1:10,000	5	0.0025
1:24,000	12	0.0144
1:50,000	25	0.0625
1:100,000	50	0.25
1:250,000	125	1.5625
1:500,000	250	6.25
1:1,000,000	500	25
1:10,000,000	5000	2500

1.2. Dimensions of the Problem

1.2.1. Precision

One of the widely accepted design principles of spatial data handling systems is that they should be able to process data without significant distortion. It is important when calculations are carried out on coordinates, for example, that the results should not be affected by lack of precision in the machine. We have seen that a figure of 0.5mm can be assumed to be typical for the resolution of

an input map document. 0.5mm is also roughly the accuracy with which an average digitizer operator can position the crosshairs of a cursor over a point or line feature. Most digitizing tables have a precision of 0.25mm or better, thus ensuring that the table itself does not introduce additional distortion as points are captured.

If we take the size of the source map sheet on the digitizing table to be 100cm by 100cm, then a precision of 0.5mm represents an uncertainty of 0.05% relative to the size of the sheet, or an uncertainty in the fourth significant digit. So in order not to introduce distortion, internal storage and processing of coordinates must be correct to at least four digits. However seven or eight decimal digits are commonplace in arithmetic calculations in spatial data handling systems, and many GISs operate at much higher precision, in effect allowing GIS users to ignore the possibility of arithmetic distortion and to assume that internal processing is carried out with infinitely high precision.

Despite this, arithmetic precision is sometimes a problem in spatial data processing, and appears in the form of unwanted artifacts. One problem is well known in connection with polygon overlay operations. It is common to find that two maps of the same theme for the same area but mapped at different scales share certain lines. For example a map of land cover at 1:250,000 should share some boundaries with a map of land cover at 1:24,000. When the two maps are overlaid the two versions of common boundaries should match perfectly. In practice this is never the case. Even if the two lines matched perfectly on the input documents, errors in registration and differences in the ways in which the digitizer operators captured the lines will ensure different digital representations in the database. Moreover since the overlay operation is carried out to high precision, the differences are treated as real and become small sliver polygons.

Several approaches have been taken to deal with the spurious polygon problem in polygon overlay, which has the annoying property that greater accuracy in digitizing merely leads to greater numbers of slivers. Some systems attempt to distinguish between spurious and real polygons after overlay, using simple rules, and to delete those which are determined to be spurious. A suitable set of rules to define spurious polygons might be:

* small in area;
* long and thin in shape (high ratio of perimeter to square root of area);
* composed of two arcs only;
* both nodes have exactly four incident arcs.

Another approach to dealing with the sliver problem is in effect to reduce the precision of the overlay operation, by requiring the user to establish a tolerance distance. Any lines lying within the tolerance distance of each other are assumed to be the same. A similar approach is often taken in digitizing, where two lines are assumed to join or 'snap' if the distance between them is less than some user-established tolerance distance.

Because a tolerance distance is in effect a reduced level of spatial resolution, all objects or features smaller than the tolerance become ambiguous or indistinguishable. For example, consider a complex vegetation cover polygon with a narrow strait or isthmus. If the width of the strait is less than the tolerance distance, it is impossible to determine from the geometry of the feature alone whether it is indeed a single polygon with a narrow strait, or two polygons. In some cases it may be possible to resolve the ambiguity if the user has already identified labels or attributes for the polygon(s); if two labels have been input, it should be clear that the feature consists of two polygons. In such instances the topology (the existence of two polygons) is allowed to resolve ambiguity in the geometry.

The potential conflict between topology and geometry is a consistent theme in spatial data handling. Franklin (1984; Franklin and Wu 1987) has written about specific instances of conflict, and about ways of resolving them. For example, a point may be given an attribute indicating that it lies inside a given polygon, but geometrically, because of digitizing error or other problems, the point may lie outside the polygon (Blakemore 1984). The conflict may be resolved by moving the point inside the polygon, or by moving the polygon boundary to include the point, or by changing the point's attributes. The first two are examples of allowing topology to correct geometry, and the third of allowing geometry to correct topology. In all cases, and particularly in the second, the implications of a change on other objects and relationships must be considered; if the polygon's boundary is moved, do any other points now change properties? Unfortunately the propagation of changes of this type can have serious effects on the overall integrity of the database.

In summary, the average user will approach a GIS or spatial data handling system with the assumption that all internal operations are carried out with infinite precision. High precision leads to unwanted artifacts in the form of spurious polygons. Moreover in reducing effective precision in such operations as digitizing and polygon closure it is common for unwanted effects to arise in the form of conflicts between the topological and geometrical properties of spatial data. The ways in which system designers choose to resolve these conflicts are important to the effective and data-sensitive application of GIS technology.

1.2.2. Accuracy

Thus far we have used examples of the distortions and errors introduced into spatial data by digitizing and processing. However if we are to take a comprehensive view of spatial data accuracy it is important to remember that accuracy is defined by the relationship between the measurement and the reality which it purports to represent. In most cases reality is not the source document but the ground truth which the source document models. The map or image is itself a distorted and abstracted view of the real world, interposed as a source document between the real world and the digital database.

We will use two terms to distinguish between errors in the source document and in the digitizing and processing steps. Source errors are those which exist in the source document, and define its accuracy with respect to ground truth. Processing errors are those introduced between the source document and the GIS product, by digitizing and processing. We will find that in general processing errors are relatively easier to measure, and smaller than source errors. Experiments with digitizing errors described in Section 3 confirm this general rule.

All spatial data without exception are of limited accuracy, and yet it is uncommon to find statements of data quality attached to such data, whether in the form of source maps, images or digital databases. The accuracy of much locational or attribute data is limited by problems of measurement, as for example in the determination of latitude and longitude, or elevation above mean sea level. In other cases accuracy is limited by problems of definition, as when a vegetation cover type is defined using terms such as 'generally', 'mostly', 'typically' and thus lacks precise, objective criteria. Locations defined by positions on map projections are limited by the accuracy of the datum, and may change if the datum itself is changed.

More subtle inaccuracies result from the way in which a source document models or abstracts reality. The transition between two vegetation cover types, which may occur in reality over some extended zone, may be represented on the source document and in the database by a simple line or sharp discontinuity. The attributes assigned to a polygon may not in fact apply homogeneously to all parts of the polygon, but may be more valid in the middle and less valid toward the edges (Mark and Csillag 1989). All of these errors result from representing spatial variation using objects; the objects are either of the wrong type for accurate representation, or used to model what is in fact continuous variation. Models such as these allow complex spatial variation to be expressed in the form of a comparatively small number of simple objects, but at a corresponding cost in loss of accuracy. Unfortunately the process of modeling has usually occurred in the definition of the source document, long before digitizing or processing in a GIS, and rarely is any useful information on levels of accuracy available.

1.2.3. Separability

Most digital spatial data models distinguish clearly between locational and attribute information. From an accuracy perspective, errors in location and attributes are often determined by quite different processes, and in these cases we term the two types of error separable. For example, a reporting zone such as a census tract may be formed from segments which follow street center lines, rivers, railroads and political boundaries. The processes leading to error in the digitizing of a river-based boundary am quite different to those typical of street center lines. Errors in imagery are similarly separable, attribute errors being determined by problems of spectral response and classification, while locational errors are determined by problems of instrument registration. The same is true to a lesser extent for topographic data, since errors in determining elevation at a point are probably only weakly dependent on errors in locating the point horizontally.

However in maps of vegetation cover, and similarly for soils or geology, where polygon objects are commonly used to model continuous variation, the two types of error are not separable, as object boundaries are derived from the same information as the attributes they separate (Goodchild 1989). The transition zone between types A and B may be much less well defined than the transition between types A and C. The process by which such maps are created gives useful clues to the likely forms of error which they contain. A forest cover map, for example, is typically derived from a combination of aerial imagery and ground truth. Polygons are first outlined on the imagery at obvious discontinuities. Ground surveys are then conducted to determine the attributes of each zone or polygon. The process may be iterative, in the sense that the ground survey may lead to relocation of the interpreted boundaries, or the merger or splitting of polygons.

1.2.4. The Ideal

The arguments in the preceding sections lead to a clear idea of how an ideal spatial database might be structured. First, each object in the database would carry information describing its accuracy. Depending on the type of data and source of error, accuracy information might attach to each primitive object, or to entire classes of objects. Accuracy might be coded explicitly in the form of additional attributes, or implicitly through the precision of numerical information.

Every operation or process within the GIS would track error, ascribing measures of accuracy to every new attribute or object created by the operation. Uncertainty in the position of a point, for example, would be used to determine the corresponding level of uncertainty in the distance calculated between two points, or in the boundary of a circle of specified radius drawn around the point.

Finally, accuracy would be a feature of every product generated by the GIS. Again it might be expressed either explicitly or implicitly in connection with every numerical or tabular result, and means would be devised to display uncertainty in the locations and attributes of objects shown in map or image form.

Of course the current state of mapping and GIS technology falls short of this ideal in all three areas. We currently lack comprehensive methods of describing error, modeling its effects as it propagates through GIS operations, and reporting it in connection with the results of GIS analysis. The remaining parts of this section describe the current state of knowledge and such techniques as currently exist for achieving a partial resolution of the error problem.

1.3. Models of Error

1.3.1. Background

With the basic introduction to accuracy and error in the previous section, we can now consider the specific issue of quality in cartographic data. This is not a simple and straightforward extension; as we will see, spatial data requires a somewhat different and more elaborate approach.

The objective is to find an appropriate model of the errors which occur in cartographic data. A model is taken here to mean a statistical process whose outcome emulates the pattern of errors observed in real digital spatial data. The first subsection considers models of error in the positioning of simple points; the second section looks at the ways this can be extended to more complex line or area features.

1.3.2. Points

The closest analogy between the classical theory of measurement and the problem of error in cartographic data concerns the location of a single point. Suppose, for example, that we wished accurately to determine the location, in coordinates, of a single street intersection. It is possible to regard the coordinates as two separate problems in measurement, subject to errors from multiple sources. If the coordinates were in fact determined by the use of a transparent roamer on a topographic sheet, then this is a fairly accurate model of reality. Our conclusion might be that both coordinates had been determined to an accuracy of 100m, or 2mm on a 1:50,000 sheet.

If the errors in both coordinates are represented by classic bell curves, then we can represent accuracy in the form of a set of ellipses centered on the point. If the accuracies are the same in each coordinate and if the errors are independent, then the ellipses become circles, again centered on the point. This gives us the circular normal model of positional error, as the two- dimensional extension of the classic error model. The error in position of a point is seen in terms of a bell-shaped surface centered over the point. The probability that any point is the true location is measured by the height of the surface of the bell over the point, and is clearly greatest at the measured location, decreasing symmetrically in all directions. Using the model we can compute the probability that the true location lies within any given distance of the measured location, and express the average distortion in the form of a standard deviation.

The Circular Standard Error is equal to the standard errors in the two coordinates, and can be portrayed by drawing a circle which passes through points representing one standard error to the left and right of the point in the x direction, and similarly above and below the point in the y direction. When the standard errors in x and y are not equal, the Circular Standard Error is approximated as the mean of the two. This approximation is valid only for small differences in the two standard errors, but it is difficult to imagine circumstances in which this would not be true. The probability that a point's true location lies somewhere within the circle of radius equal to the Circular Standard Error is 39.35%. The Circular Map Accuracy Standard (CMAS) requires that no more than 10% of the errors on a map will exceed a given value. For example, with a CMAS of 1mm, in order to meet the standard no more than 10% of points should be more than lmrn from their true positions. Under the circular normal model a radius of 2.146 times the circular standard error will contain 90% of the distribution, with 10% lying outside. The relationship between the CMAS and the circular standard error is therefore a ratio of 2.146.

These indices have been incorporated into many of the widely followed standards for map accuracy. For example, the North Atlantic Treaty Organization (NATO) standards rate maps of scales from 1:25,000 to 1:5,000,000 as A, B, C or D as follows:

A: CMAS = 0.5mm (e.g. 12.5m at 1:25,000)

B: CMAS = I.0mm (e.g. 25m at 1:25,000)

C: CMAS determined but greater than I.0mm

D: CMAS not determined.

Many other mapping programs use CMAS as the basis for standards of horizontal or planimetric accuracy, and use similar values.

1.3.3. Lines and areas: the Perkal band

In vector databases lines are represented as sequences of digitized points connected by straight segments. One solution to the problem of line error would therefore be to model each point's accuracy, and to assume that the errors in the line derived entirely from errors in the points. Unfortunately this would be inadequate for several reasons. First, in digitizing a line a digitizer operator tends to choose points to be captured fairly carefully, selecting those which capture the form of the line with the greatest economy. It would therefore be incorrect to regard the points as randomly sampled from the line, or to regard the errors present in each point's location as somehow typical of the errors which exist between the true line and the digitized representation of it.

Secondly, the errors between the true and digitized line are not independent, but instead tend to be highly correlated (Keefer, Smith and Gregoire 1988; Amrhein and Griffith 1987). If the true line is to the east of the digitized line at some location along the line, then it is highly likely that its deviation immediately on either side of this location is also to the east by similar amounts. Much of the error in digitized lines results from misregistration, which creates a uniform shift in the location of every point on the map. The relationship between true and digitized lines cannot therefore be modeled as a series of independent errors in point positions.

One commonly discussed method of dealing with this problem is through the concept of an error band surrounding the line of width epsilon, known as the Perkal epsilon band (Perkal 1956, 1966; Blakemore 1984; Chrisman 1982). The model has been used in both deterministic and probabilistic forms. In the deterministic form, it is proposed that the true line lies within the band with probability 1.0, and thus never deviates outside it. In the probabilistic form, on the other hand, the band is compared to a standard deviation, or some average deviation from the true line. One might assume that a randomly chosen point on the observed line had a probability of 68% of lying within the band, by analogy to the percentage of the normal curve found within one standard deviation of the mean.

Some clarification is necessary in dealing with line errors. In principle, we are concerned with the differences between some observed line, represented as a sequence of points with intervening straight line segments, and a true line. The gross misfit between the two versions can be measured readily from the area contained between them, in other words the sum of the areas of the spurious or sliver polygons. To determine the mismatch for a single point is not as simple, however, since there is no obvious basis for selecting a point on the true line as representing the distorted version of some specific point on the observed line. Most researchers in this field have made a suitable but essentially arbitrary decision, for example that the corresponding point on the true line can be found by drawing a line from the observed point which is perpendicular to the observed line (Keefer, Smith and Gregoire 1988). Using this rule, we can measure the linear displacement error of any selected point, or compute the average displacement along the line.

Although the Perkal band is a useful concept in describing errors in the representation of complex objects and in adapting GIS processes to uncertain data, it falls short as a stochastic process model of error. An acceptable model would allow the simulation of distorted versions of a line or polygon, which the Perkal band does not, and would provide the basis for a comprehensive analysis of error.

1.3.4. Alternatives to the Perkal band

Goodchild and Dubuc (1987) proposed a model based on an analogy to the effect of mean annual temperature and precipitation on life zones. We first generate two random fields, using one of a number of available methods, such as the fractional Brownian process, turning bands or Fourier transforms (Mandelbrot 1982). The autocovariance structure of the fields can be varied to create a range of surfaces from locally smooth to locally rugged. Imagine that one field represents mean annual temperature and the other, annual precipitation.

Holdridge et al. (1971) have proposed a simple two-dimensional classifier which, given temperature and precipitation, yields the corresponding ecological zone. By applying such a classifier to the two fields, we obtain a map in which each pixel has been classified into one of the available zones. If the pixels are now vectorized into homogeneous areas, the map satisfies the requirements

of many types of area class maps: the space is exhausted by nonoverlapping, irregularly shaped area objects, and edges meet in predominantly three-valent vertices. On the other hand if a single field had been used with a one-dimensional classifier, the result would have the unmistakable features of a contour or isopleth map. To simulate the influence of the cartographer, Goodchild and Dubuc (1987) applied a spline function to the vectorized edges, and selectively removed small islands.

The model has interesting properties which it shares with many real datasets of this class. Because the underlying fields are smooth, classes can be adjacent in the simulated map only if they are adjacent in the classifier, so certain adjacencies are much more common than others. The response of an edge to a change in one of the underlying fields depends on the geometry of the classifier: it is maximum if the corresponding edge in the classifier space is perpendicular to the appropriate axis, and minimum (zero) if the edge is parallel to the axis. So distortion or error can be simulated by adding distortion to the underlying fields.

The model successfully simulates the appearance of area class maps, including maps of vegetation cover, and is useful in creating datasets under controlled conditions for use in benchmarking spatial databases and GIS processes, and for tracking the propagation of error. On the other hand the large number of parameters in the model make it difficult or impossible to calibrate against real datasets. Parameter values would have to be established for the underlying fields, the distorting field(s), the classifier, and the spline function used to smooth vectorized edges.

Goodchild and Wang (1988) describe an alternative model based on an analogy to remote sensing. Suppose that the process of image classification has produced an array of pixels, and that associated with each pixel is a vector of probabilities of membership in each of the known classes. For example the vector (0.3,0.3,0.41 would indicate probabilities of 0.3, 0.3 and 0.4 of membership in classes A, B and C respectively. In practice we would expect the proportion of non-zero probabilities to be small, allowing the vectors to be stored efficiently.

We now require a process of realizing pixel classes such that (1) the probabilities of each class across realizations are as specified, and (2) there is spatial dependence between pixels in any one realization. The degree of spatial dependence win determine the size of homogeneous patches which develop. With high spatial dependence, a given pixel will belong to large patches in each realization: in 30% of realizations the example pixel will be part of a patch of class A, 30% B and 40% C.

The vectors of probabilities required by this process are readily obtainable from many remote sensing classifiers, and can also be found in the legends of many maps of vegetation cover or soil class. Conventionally, pixels are classified by maximum likelihood even though the classifier yields a complete vector. This results in the loss of valuable information on uncertainty, and leads to severe bias in derived estimates of area, particularly for large patches. The model has only one parameter, defining the level of spatial dependence. Its value might be established by calibration against ground truth, or might be set to reflect expectations about patch size and map complexity.

1.3.5. Models for errors in areal estimates from dot and pixel counting

One of the traditional methods of measuring area from a map involves placing an arTay of grid cells or dots over the area to be measured, and counting. In the past, the method has been used extensively in forest inventory work. In principle this process is similar to that of obtaining the area of a patch from an image by counting the pixels which have been classified as belonging to or forming the patch. The accuracy of the area estimate clearly depends directly on the density of dots or the pixel size, but so does the cost of the operation, so it would be useful to know the precise relationship in order to make an informed judgment about the optimum density or size.

The literature on this topic has been reviewed by Goodchild (1980). In essence two extreme cases have been analyzed, although intermediates clearly exist. In the first the area consists of a small number of bounded patches, often a single patch; in the second, it is highly fragmented so that the average number of pixels or dots per fragment of area is on the order of one or two. We refer to these as cases A and B respectively. Case A was first analyzed by Frolov and Maling (1969), and later by Goodchild (1980). The limits within which the true area is expected to lie 95% of the time, expressed as a percentage of the area being estimated, are given by:

$$1.03\ (kn)^{1/2}\ (SD)^{-3/4} \qquad (1)$$

where:

n is the number of patches forming the area;
k is a constant measuring the contortedness of the patch boundaries, as the ratio of the perimeter to 3.54 times the square root of area (k=1 for a circle);
S is the estimated area; and
D is the density of pixels per unit area.

The results for Case B follow directly from the standard deviation of the binomial distribution, since this case allows us to assume that each pixel is independently assigned. The limits within which the true area is expected to lie 95% of the time, again as a percentage of the area being estimated, are given by:

$$1.96\ [1-S/S0]^{1/2}\ (S/D)^{1/2} \qquad (2)$$

where S0 is the total area containing the scattered patches.

Error rises with the 3/4 power of cell size in case A, but with the 1/2 power in case B. Thus a halving of cell size will produce a more rapid improvement in error in case A, other things being equal, because only cells which intersect the boundary of the patch generate error in case A, whereas all ceRs are potentially sources of error in case B, irrespective of cell size.

1.3.6. Error in images

Images such as those derived from remote sensing are composed of pixels (picture elements) of uniform size and shape, with associated measures of reflected or emitted radiation. After classification, each pixel is assigned to one of a number of classes, often of land use or land cover. Unlike the cartographic case, there are no objects or features to be located, and accuracy is simply a function of the errors in the assignment of classes to each pixel. The standard method of measuring accuracy in a classified image is to compare the classes assigned to a sample of pixels to the true classes on the ground ('ground truth') and express the result in the form of a table, the rows representing the assigned class and the columns the ground truth.

Pixels which fall on the diagonal of the table are correctly classified; pixels which fall off the diagonal in a column are termed 'errors of omission' since the true value is omitted from the assigned class; and pixels which fall off the diagonal in a row am termed 'errors of omission' since they appear as false occurrences of a given class in the data. The contents of the table can be summarized in statistics such as the percentage of cells correctly classified, or using Cohen's Kappa statistic, which allows for correct classification by chance (see Congalton, Oderwald and Mead 1983; van Genderen and Lock 1977; van Genderen, Lock and Vass 1978; Greenland, Socher and Thompson 1985; Mead and Szajgin 1982; Rosenfield 1986; Rosenfield and Fitzpatrick-Lins 1986). These methods are used in Section 3.

1.4. Summary

As we have seen, techniques for dealing with uncertainty in spatial data are much better developed in some areas than others. Uncertainties in point locations are comparatively easy to deal with, and a significant proportion of geodetic science is devoted to dealing with the issue of accuracy in control networks. Substantial progress has been made in modeling the error introduced by digitizing, and in predicting its effects on the measures of perimeter and area of objects (Griffith 1989; Chrisman and Yandell 1988). But the more general problem of modeling the accuracy of spatial data with respect to ground truth remains. In part this is because of the complexity of the processes involved, and in part because many ground truth definitions are themselves uncertain. But in addition, we have seen how the representation of spatial variation as objects acts in many cases to make error modeling more difficult, simply because of the nature of the object data model. Both of the models of error in area-class maps presented above are defined first in terms of continuous variation, using the raster data model, and then used as the basis for deriving uncertainty in objects. If the accuracy issue leads us to question the use of traditional data models then any progress will certainly be slow.

The accuracy of spatial databases is the topic of the first research initiative of the National Center for Geographic Information and Analysis (NCGIA), which began with a meeting of specialists in Montecito, CA in December 1988. The collection of papers from

that meeting has been published (Goodchild and Gopal 1989) and provides a broad overview of the accuracy issue in spatial data handling generally. The meeting identified an eleven- point research agenda: data structures and models; models of error and distortion; error propagation; product uncertainty and sensitivity; risk analysis; accuracy concerns among users and agencies; experimentation and measurement; error reduction methods; interpolation and surface modeling; aggregation, disaggregation and modifiable areal units; regularity and stability.

If accuracy is a problem in spatial data handling because of the high precision of the handling system, then one rational approach would be to reduce precision to match accuracy. In effect this is what happens in a raster system. Dutton (1984 1989; see also Goodchild and Yang 1989) makes this point, and proposes a tesseral scheme for global data that would replace common coordinate referencing with a finite-resolution hierarchical key.

There has been substantial progress in recent years in understanding the propagation of uncertainty that occurs in spatial data handling. Newcomer and Szajgin (1984) and Veregin (1989) have discussed error propagation during simple Boolean overlay; Lodwick (1989; Lodwick and Monson 1988) and Heuvelink et al. (1989) have analyzed the sensitivity of weighted overlay results to uncertainty in the input layers and weights; and Arbia and Haining (1990) have analyzed a general model of uncertainty in raster data. However overlay is perhaps the most simple of the primitive spatial data handling operations. Much more research is needed on the effects of buffering (dilating) uncertain objects, and of changing from one data model to another, e.g. raster/vector conversion.

If traditional map data models tend to give a misleading impression of the reliability of data, it is not surprising that many cartographic products fail to make the user aware of uncertainties. The move to standards of data quality is a significant step toward greater awareness of the reliability of spatial data, and includes concepts of lineage, consistency and completeness as well as the more statistical issues discussed in this section. It is particularly important as GIS users continue to apply spatial data to purposes for which they may not have been designed. It is also important that standards of data quality be developed in specific application areas, such as vegetation cover mapping.

2. AN EVALUATION OF THE CALVEG MAP OF THE NATURAL VEGETATION IN CALIFORNIA

In this section we describe an error analysis of the CALVEG map of vegetation in California. We chose this map because it is the only recent, statewide vegetation map of California and because it has been used by CDF for statewide resource assessments. Our intent is not to level criticism at this map or those who created it, as all small-scale vegetation maps suffer similar errors, but to use the map to demonstrate the types of errors that can affect vegetation maps and to test some methods for assessing those errors. Our analyses proceed from conventional contingency table comparisons of map and field samples to analysis of the spatial properties of the map errors and finally to a test of the use of ancillary environmental data to predict those errors.

2.1. CALVEG Vegetation Classification and Mapping

CALVEG is a hierarchical classification system of actual vegetation designed to assess vegetation-related resources throughout California. The system was devised in the late 1970's by the California Region of the U.S. Forest Service to describe and map natural vegetation in the state. A statewide map was produced at the series level, with series defined by the dominant overstory species of the community (e.g., Ponderosa Pine series).

CALVEG mapping was done between 1979 and 1981 by U.S. Forest Service personnel by photointerpretation of color infrared prints of Landsat Multispectral Scanner (MSS) imagery acquired between 1977 and 1979 (Matyas and Parker, 1980). Image interpretation was guided by existing soil and vegetation maps, via 5,000 miles of field checking and by personal contact with vegetation experts throughout the state (Matyas and Parker 1980). The nominal minimum mapping unit was 400-800 acres, but the spatial resolution of the resulting map was very coarse. Average polygon size of the map mosaic (i.e., with boundaries due to map edges deleted) is 38,000 acres for the entire state. The map was field checked at the time of its compilation (Wendy Matyas, personal communication, 1989), but estimates of its accuracy were not published. The map's editors asserted that it was intended only for broad scale resource assessments and not for detailed planning (Wendy Matyas, personal communication).

2.2. Field Comparison of CALVEG to Other Small-scale Vegetation Maps

We collected field observations of vegetation cover at 78 sample locations in Southern California to compare CALVEG to Kuchler's map of Potential Natural Vegetation in California (Kuchler 1977) and to the California Condor Habitat Map (Davis et al. 1989). (See Duncan 1990 and Duncan et al. 1990 for details). Our purpose was to compare the types and rates of errors that affected these maps within a region, based on field samples at an appropriate spatial scale that were jointly classified into all three vegetation classification schemes. Furthermore, we wanted to test whether complementary properties of these maps could be exploited to derive better vegetation information for the region. Methods and results are summarized below.

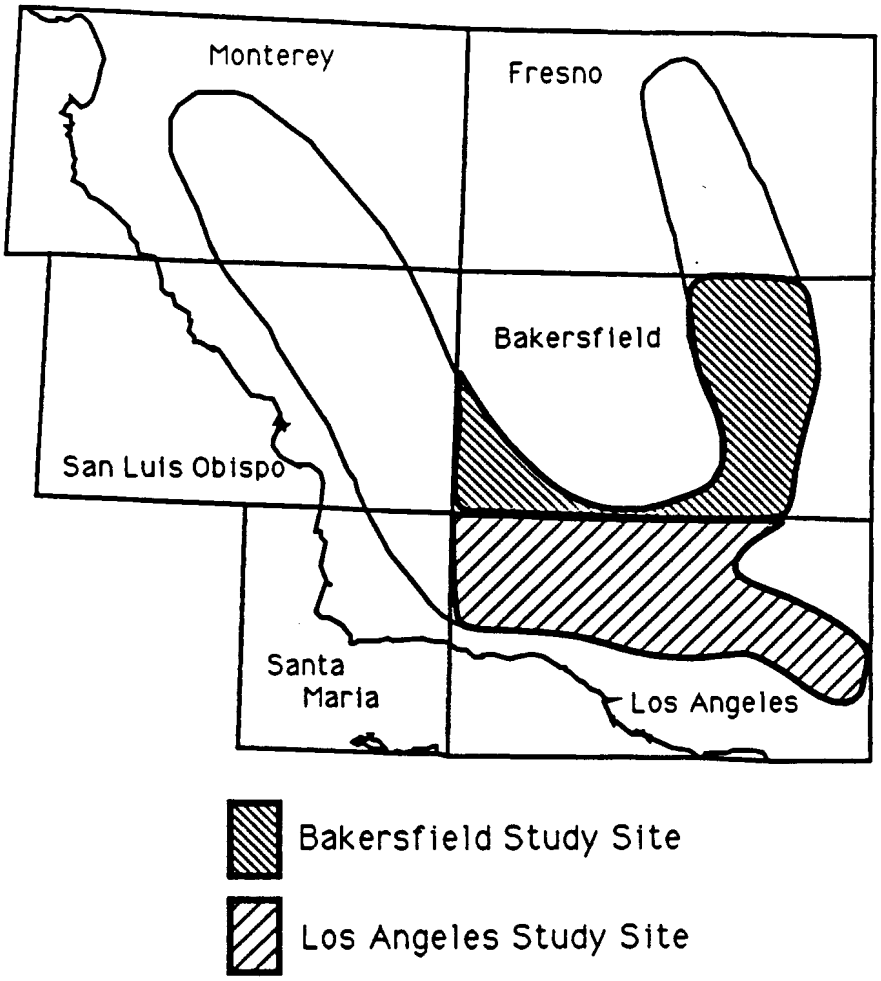

Figure 1. Study area for field comparisons of CALVEG, Kuchler and Condor Habitat maps of natural vegetation. 41 samples were located in shaded region of the Los Angeles quadrangle and 36 were located in the shaded region of the Bakersfield quadrangle. The polygon encloses the recent historical range of the California condor.

Vegetation maps were combined and analyzed for portions of the Los Angeles and Bakersfield quadrangles of southern California (Figure I).

The 912,015 ha study area in the Los Angeles quad includes the mountainous areas of the Los Padres National Forest, and is covered by grassland, chaparral and woodland vegetation. The 681,157 ha region of the Bakersfield quad included grassland, chaparral and mixed broadleaf and conifer woodland. The digital version of CALVEG, which we obtained from CDF&FP, was produced by scanning of the 1:250,000 mylar manuscript maps. The Condor Habitat Map was already available at UCSB. That portion of Kuchler's 1:1,000,000 map of potential natural vegetation covering the southern half of the state was digitized using ARC/INFO. The classification systems differed among the maps, so they could only be compared at higher levels of aggregation.

Seventy-eight field samples were located at random distances along unpaved roads in the Los Padres and Sequoia National Forests. Sample locations to the nearest 50-100 m were obtained using a portable Loran Navigational System calibrated to local benchmarks. In an attempt to approach the Minimum Mapping Unit (MMU) of the Condor and CALVEG maps, only locations in homogeneous stands of at least 25 hectares in extent were recorded. Where vegetation mosaics were observed, the two most extensive vegetation types were coded as "primary" and "secondary" based on their relative areal extent. This allowed us to consider map accuracy somewhat more flexibly, in that the map could be tested for agreement with actual vegetation that was either dominant or at least well represented in the area. The sample size of 78 was too small to quantify the class-specific accuracy of any of the maps, but was useful in comparing overall rates of errors that affected these maps within a limited region.

Both Condor and CALVEG maps were produced by interpreting 1:250,000 satellite prints, but the Condor project utilized 1986 Thematic Mapper data (a false color composite of bands 3,4 and 5) instead of MSS data. Also vegetation was mapped at greater spatial detail in the Condor Habitat Map than in CALVEG, although using a simpler, 14-class physiognomic classification system. Using that 14-class system, the Condor map agreed with primary or secondary vegetation class observed in the field at 57/78 or 73% of the sites (Table 2). Using the same classification scheme, CALVEG was in agreement at only 39/77 or 50% of the sites (Table 3). Surprisingly, Kuchler's smaller scale map of potential vegetation agreed with the primary or secondary field vegetation data at 41n8 or 53% of the sites (Duncan, 1990). CALVEG errors in predicting vegetation sub-formation thus appeared due not only to problems of generalization, which affected both the Kuchler and CALVEG maps, but also to errors of polygon misclassification.

When field samples were classified by CALVEG type, map and ground samples agreed at only 19n8 sites (24%). This level of agreement is especially low when one considers that the map was considered correct if it agreed with either the primary or secondary vegetation cover observed in the field. Most of the confusion was due to errors of map commission in the Chamise chaparral and Mixed conifer/Pine types (Table 4). In particular, 8/13 samples from the foothills of the southern Sierra Nevada that were mapped as chamise chaparral were observed to be blue oak woodland. 10/14 samples from the Transverse Ranges mapped as chamise chaparral also proved to be blue oak woodland or other types.

There are probably many sources contributing to error in the CALVEG map, including generalization, polygon misclassification and processing errors. Misclassifications could occur from simple errors in labeling during the drafting or digitizing processes. Some errors of this type were detected by searching the map for logical inconsistencies. For instance one polygon in the Bakersfield quadrangle that was labeled on the original mylar as Jeffrey pine was located within a creosote bush polygon. Jeffrey pine is a conifer typically found at middle elevations of the Sierra Nevada mountains, whereas creosote bush is characteristic of most of the Mojave Desert. The mostly likely explanation is that a cartographer mistook Jeffrey pine for Joshua tree, which has a similar label and does co-occur with creosote bush. Other sources of error were investigated using the larger set of ground samples provided by the FIA data, as discussed in the next section.

Table 2. Contingency table comparison of the Condor habitat map versus field observations in the 1:250,000 Los Angeles and Bakersfield quadrangles. The vegetation classification scheme used to map Condor habitats was considerably simpler than the CALVEG system.

	CONDOR HABITAT MAP													
FIELD	Urb	Ag	Ba	He	SCh	HCh	CW	MW	BW	CF	MF	BF	Total	%Agree
Urb													0	
Ag													0	
Bare				1	1								2	0
Herb	1			11									12	92
Sft Chap				1	4								5	80
Hrd Chap						24							24	100
Con Wood							8	1			1		10	67
Mxd Wood		1						7					8	88
Con Forest				2							3		5	0
Mxd Forest					1	2					3		6	50
Brdlf Forest						1		1	1	1			4	0
Total	1	1	1	15	5	27	8	9	3	0	8	0	78	

Agree 73.1%
Expected 17.6%
Kappa 67.3%

Legend

Urb Urban	Ag Agriculture	
He Herbaceous	SCh Soft Chaparral	HCh Hard Chaparral
CW Conifer woodland	MW Mixed Woodland	BW Broadleaf Woodland
CF Conifer Forest	MF Mixed Forest	BF Broadleaf Forest

Table 3. Contingency table comparison of the CALVEG map recoded to Condor habitat types versus field observations in the 1:250,000 Los Angeles and Bakersfield quadrangles. See Table 2 for the abbreviation code.

	CALVEG MAP									
FIELD	Urb/Ag	Bare	Hrb	SCh	HCh	CW/CF	MW/MF	BW/BF	Total	%Agree
Urb/Ag									0	
Bare					2				2	0
Hrb			2		4				6	67
SCh			1		1	1			3	0
HCh	2		1		18	2		2	25	72
CW/CF						15	1	1	17	88
MW/MF					3	10	1	2	16	6
BW/BF					4	1		3	8	38
Total	2	0	4	0	32	29	2	8	77	

Agree 50.7%
Expected 23.8%
Kappa 35.2%

Table 4. Contingency table comparison of CALVEG versus field observations in the 1:250,000 Los Angeles and Bakersfield quadrangles. See Table 5 for abbreviations to CALVEG types.

	CALVEG MAP																
FIELD	UA	HG	CA	CS	BC	BR	QD	QW	QA	PE	PP	JP	MP	WF	TP	Total	% Agree
UA								1								1	0
Ba		3	1													4	0
HG		1	2	1												4	25
CC		1							1							2	0
CA	2		5													7	71
CW			3													3	0
CS	1		2										1		2	6	0
BR		1								1			1			3	0
QD			8				5									13	38
QW			1					1			1					3	33
QA			1													1	0
QC			3													3	0
QK											2					2	0
PE							1						1			2	0
PP			1								2		5			8	25
JP														2		2	0
MP			1				1				3	2	5	2		14	36
Total	3	6	28	1			7	2	1	1	8	2	13	4	2	78	

Agree 24.4%
Expected 9.5%
Kappa 16.4%

Table 5. List of abbreviations for CALVEG and FIA vegetation types.

Formation	Code	CALVEG Type
Conifer forest/woodland	CP	Coulter Pine
	DF	Douglas Fir/Bigcone Spruce
	DP	Douglas Fir/Pine
	GF	Grand Fir
	JP	Jeffrey Pine
	KP	Knobcone Pine
	LP	Lodgepole Pine
	MF	Mixed Conifer/Fir
	MP	Mixed Conifer/Pine
	PE	Pinyon Pine
	PJ	Pinyon-Juniper
	PM	Pishop Pine
	PP	Ponderosa Pine
	PR	Monterey Pine
	RD	Redwood/Douglas Fir
	RF	Red Fir
	RW	Redwood
	SG	Sitka Spruce/Grand Fir
	WF	White Fir
	WJ	Western Juniper
Broadleaf Forest/Woodland	LA	Tanoak/Madrone
	QA	Coast Live Oak
	QB	?
	QC	Canyon Live Oak
	QD	Blue Oak
	QG	Oregon Oak
	QH	?
	QK	Black Oak
	QL	Valley Oak
	QM	?
	QR	?
	QT	Quaking Aspen
	QU	Buckeye
	QW	Interior Live Oak
Shrublands	BA	Blackbrush
	BM	?
	BR	?
	BS	Great Basin Sagebrush
	CA	Chamise
	CC	Ceanothus
	CG	Greenleaf Ceanothus
	CI	Deerbrush
	CJ	?
	CK	Scotchbroom
	CL	Wedgeleaf Ceanothus
	CM	Redshank
	CS	Scrub Oak
	CT	?
	CV	Tobacco Brush
	CW	Manzanita
	CX	?
Herbaceous	HG	Annual Grassland
	HM	Perennial Grassland
	MN	Mule's Ear

2.3. Contingency Table Analysis of CALVEG using FIA data

Both FIA photoplot and ground data were used to assess the accuracy of CALVEG. Photoplot data consist of 56,973 photo-interpreted points produced by the U.S. Forest Service Pacific Northwest Forest and Range Experiment Station in Portland, Oregon, (McKay, 1987) as part of a statewide Forest Inventory and Assessment (FIA). A systematic random sample was used to select sites, with an average grid spacing of 0.85 miles. All land in California outside of the National Forests was sampled. This dataset, therefore, provides better coverage of the non-timber lands of the California study site than the timber inventory plots do. However, these points were photo interpreted, not field checked, so they are more subject to interpretation errors.

FIA also conducted intensive field surveys at a large subset of the photointerpreted points. They coded each field plot record into a corresponding class of the CALVEG system and then compared the plot to the corresponding location in the digital CALVEG map. We should emphasize that both field and photo plots sampled areas much smaller than the nominal MMU of CALVEG, and so are not a strict test of the map's accuracy. Again, our focus is on the methodology of error assessment rather than the specific errors affecting CALVEG.

2.3.1. Contingency Comparison of CALVEG and FIA Field Data

We recoded 1347 field plots for comparison with CALVEG. 54 CALVEG types were encountered in the field compared to 37 types that were actually mapped (Table 6). The full contingency table is large and sparse, and there is not one-to-one correspondence between FIA classes and CALVEG classes, so we have not statistically analyzed map accuracy at this level. To help study the map errors, table rows and columns have been sorted by formations into conifer woodlands and forests, broadleaf woodland and forest, shrublands and grasslands.

Most samples fall into the upper left portion of the table, that is mapped and observed as conifer woodland and forest. Notable sources of commission errors between conifer and non-conifer types include the frequent occurrence of Canyon live oak (QC) and Black oak (QK) types in polygons mapped as Mixed Conifer/Pine (36/297, 12. 1 %) and the occurrence of Quaking aspen (QT) in areas mapped as Douglas Fir (DF) (16/73, 21.9%).

Frequent omission errors include the occurrence of Douglas Fir (DF) in areas mapped as Tanoak/Madrone (LA) or Black oak (QK) (30/127, 23.6%) and the occurrence of Ponderosa Pine (PP) in polygons mapped as Manzanita chaparral (CW) (10/103, 9.7%). These errors are among types that occur on similar sites within the same climatic regions, suggesting that the errors may be a function of map generalization rather than polygon misidentification.

A simpler and more readily analyzed contingency table was produced by collapsing nonconifer types to the three formation classes (Table 7). Marginal class accuracies (sometimes referred to as map class versus ground class accuracies, or producer versus consumer accuracies) were calculated for types with sample sizes larger than 4 and occurring in both FIA and CALVEG classification schemes.

Based on those types, the overall map accuracy was 38%, compared to an expected accuracy of 13% by chance alone. The adjusted accuracy or Kappa statistic for the table is 29%.

Table 7 highlights considerable confusion in mapping some conifer classes. Douglas Fir (DF) was mapped with relatively high consumer accuracy (57%) but low producer accuracy (33%) due to high rates of omission error with Mixed Conifer Pine (MP), Redwood/Douglas Fir (RD) and Hardwoods (Hdwd). In contrast, Redwood/Douglas Fir was mapped with very high producer accuracy in CALVEG (84%), but with low consumer accuracy due to confusion with Redwood (RW) and Douglas Fir (DF) (52%). Mixed Conifer/Fir (MF) was mapped with 53% consumer accuracy, the main confusion being with Jeffrey Pine (JP) and Mixed Conifer/Pine (W). Producer accuracy was low (30%) due to the high rate of confusion with Mixed Conifer/Pine (W). Ponderosa Pine (PP) was mapped with low consumer accuracy (26%) and producer accuracy (19%). Ground plots in Ponderosa Pine were frequently mapped as Jeffrey Pine (JP), Mixed Conifer/Pine (MP), Hardwood or Shrubland types. Areas mapped as Ponderosa Pine were often coded as Mixed Conifer/Pine or Mixed Conifer/Fir in the field.

One way to help display relationships between ground and map classes is to sort the rows and columns of the confusion matrix in a way that orders ground classes based on their distribution in map classes, and orders map classes based on the composition of their field plots. To this end, rows and columns of the table were sorted based on two-step cluster analysis (agglomerative, average link, euclidean distance) of the rows and then the columns of the original matrix (Table 8).

Table 6. Contingency table of CALVEG map (columns) versus FIA field plots (rows).

TYPE	CP	DF	DP	JP	MF	MP	PJ	PP	PR	RD	RF	RW	SG	WJ	LA	QA	QC	QD	QG	QK	QL	QW	BS	CA	CE	CG	CM	CO	CS	CW	CX	DL	SS	HG	HM
CP	0	0	0	0	0	0	0	0	0	3	0	0	0	0	0	0	0	0	0	0	0	0	0	0	0	0	0	0	0	0	0	0	1	0
DF	0	42	2	0	2	13	0	1	0	25	0	0	0	0	16	2	2	1	2	14	0	0	0	0	0	0	0	1	0	1	0	0	3	0
DP	0	2	4	1	0	16	0	0	1	0	0	0	0	0	0	0	0	0	0	1	0	0	0	0	0	0	2	0	0	0	0	0	0	0
GF	0	1	0	0	0	0	0	0	0	1	0	0	0	0	0	0	0	0	0	0	0	0	0	0	0	0	0	1	0	0	0	0	0	0
JP	0	0	0	4	10	4	0	2	0	0	1	0	0	0	0	0	2	0	0	0	0	1	3	0	0	0	3	0	0	0	0	0	0	0
KP	0	0	0	0	0	1	0	1	0	0	0	0	0	0	0	0	1	0	0	0	0	0	0	0	1	0	0	0	0	0	0	0	0	0
LP	0	0	0	0	1	1	0	0	0	0	0	0	0	0	0	0	0	0	0	0	0	0	0	0	0	0	0	0	0	0	0	0	0	0
MF	0	0	1	2	53	71	0	13	0	0	10	0	0	0	0	0	5	2	0	2	0	0	0	0	4	1	1	0	0	10	0	0	0	0
MP	0	0	0	6	17	67	0	12	0	0	2	0	0	1	0	0	2	0	3	3	0	2	0	0	1	3	1	0	0	1	0	0	0	0
PE	0	0	0	0	0	0	1	0	0	0	0	0	0	0	0	0	0	0	0	0	0	0	0	0	0	0	0	0	0	0	0	0	0	0
PJ	0	0	0	1	1	1	6	0	0	0	0	0	0	1	0	0	0	0	0	0	0	0	2	0	0	0	0	0	0	0	0	1	0	0	2
PM	0	0	0	0	0	0	0	0	0	1	0	0	0	0	0	0	0	0	0	0	0	0	0	0	0	0	0	0	0	0	0	0	0	0
PP	3	1	0	8	2	40	1	20	0	0	1	0	0	1	0	0	4	2	1	0	0	3	2	1	0	1	1	0	0	11	0	0	0	0
RD	0	4	0	0	0	0	0	0	0	100	0	0	0	0	0	4	0	0	0	5	0	0	0	0	0	0	0	6	0	0	0	0	0	0
RF	0	0	0	0	3	3	0	0	0	0	7	0	0	0	0	0	0	0	0	0	0	0	0	0	0	0	0	0	0	0	0	0	0	0
RW	0	0	0	0	0	0	0	0	0	35	0	0	0	0	2	9	4	0	0	0	0	0	0	0	0	0	0	3	0	0	0	0	0	0
SG	0	0	0	0	0	0	0	0	0	0	0	0	2	0	0	0	0	0	0	0	0	0	0	0	0	0	0	0	0	0	0	0	0	0
WF	0	0	0	0	5	3	0	1	0	0	3	0	0	0	0	0	1	0	0	0	0	1	1	0	0	0	1	0	0	0	0	0	0	0
WJ	6	0	0	0	1	3	0	0	0	0	0	0	0	5	0	0	1	0	0	0	0	0	21	0	0	0	1	0	0	0	0	2	0	0	1
QA	0	0	0	0	0	1	0	0	0	0	0	0	0	0	1	11	0	3	0	0	1	0	0	3	0	0	0	1	0	0	1	0	0	0
QB	0	0	0	0	0	0	0	0	0	0	0	0	0	0	0	1	0	1	0	0	0	0	0	0	0	0	0	0	0	0	0	0	0	0
QC	0	0	0	0	0	20	1	2	0	2	0	0	0	0	4	3	3	1	1	3	0	4	0	0	0	0	3	0	0	2	0	0	0	0
QD	0	0	0	0	0	5	0	2	0	0	0	0	0	0	0	1	3	50	0	1	1	11	0	8	0	0	0	0	0	10	0	0	0	4	0
QG	0	2	1	2	0	6	0	5	0	5	0	0	0	0	12	1	1	1	2	4	0	1	1	0	0	0	1	0	0	0	0	0	0	0	0
QH	0	2	0	0	0	0	0	1	0	0	0	0	0	0	1	0	0	0	0	0	0	0	0	0	0	0	0	0	0	0	0	0	0	0	0
QK	0	2	0	0	0	16	0	3	0	1	0	0	0	0	1	1	0	4	0	6	0	2	0	0	0	0	1	0	0	4	0	0	0	1	0
QL	0	0	0	0	0	2	0	0	0	0	0	0	0	1	0	0	0	1	0	1	0	0	0	0	0	0	0	0	0	0	0	0	0	0	0
QM	0	0	0	0	0	0	0	0	0	0	0	0	0	0	0	0	0	0	0	1	0	0	0	0	0	0	0	0	0	0	0	0	0	0	0
QO	0	0	0	0	0	1	0	0	0	0	0	0	0	0	0	0	0	0	0	0	0	0	0	0	0	0	0	0	0	0	0	0	0	0	0
QR	0	0	0	0	0	0	0	0	0	3	0	0	0	0	0	0	0	0	0	0	0	0	0	0	0	0	0	0	0	0	0	0	0	0	0
QT	0	16	0	3	0	1	0	0	0	12	0	1	0	0	10	3	0	0	0	1	0	0	0	0	0	0	0	1	0	0	0	0	1	0
QU	0	0	0	0	0	0	0	0	0	1	0	0	0	0	0	1	0	0	0	0	0	0	0	0	0	0	0	0	0	0	0	0	0	0	0
QW	0	0	0	0	0	10	0	1	0	0	0	0	0	0	0	1	1	9	0	4	0	5	0	3	0	0	0	0	0	3	0	0	0	2	0
UA	0	0	0	0	0	0	0	1	0	0	0	0	0	0	0	0	0	0	0	0	0	0	0	0	0	0	0	0	0	1	0	0	0	0	0
BA	0	0	0	0	1	1	0	0	0	0	0	0	0	0	1	0	0	0	0	0	0	0	0	0	0	0	0	0	0	0	0	0	0	0	0
BM	0	0	0	0	1	1	0	0	0	0	0	0	0	0	0	0	0	0	0	0	0	0	2	0	0	0	0	0	0	0	0	0	0	0	0
BR	1	0	0	0	0	0	0	0	0	0	0	0	0	0	0	0	0	0	0	0	0	1	0	0	0	0	0	0	0	0	0	0	0	0	0
BS	1	0	0	1	0	0	0	0	0	0	0	0	0	0	0	0	0	0	0	0	0	0	0	0	0	0	0	0	0	0	0	0	0	0	0
CA	0	0	0	0	0	1	0	4	0	0	0	0	0	0	2	7	0	12	0	2	0	1	0	10	0	0	1	2	2	0	0	0	0	2	0
CC	0	0	0	0	0	0	0	0	0	0	0	0	0	0	0	0	0	1	0	0	0	0	0	0	0	0	0	0	0	0	0	0	0	0	0
CG	0	0	0	2	1	3	0	3	0	0	1	0	0	0	0	0	0	0	0	0	0	1	0	0	0	0	0	0	0	1	0	0	0	0	0
CI	0	0	0	0	0	0	0	0	0	0	0	0	0	0	0	0	0	0	0	0	0	0	0	0	0	0	1	0	0	0	0	0	0	0	0
CJ	0	0	0	0	0	0	0	2	0	0	0	0	0	0	0	0	0	2	0	0	0	0	0	0	0	0	0	0	0	0	0	0	0	0	0
CK	0	0	0	0	0	0	0	0	0	1	0	0	0	0	1	0	0	0	0	0	0	0	0	0	0	0	0	1	0	0	0	0	1	0	0
CL	0	0	0	0	1	1	1	3	0	0	0	0	0	0	0	0	2	1	0	0	0	1	0	1	0	0	1	0	0	0	0	0	0	0	0
CM	0	0	0	0	0	1	0	0	0	0	0	0	0	0	0	0	0	0	0	0	0	0	0	0	0	0	0	0	0	0	0	0	1	0	0
CS	0	0	0	0	0	1	0	0	0	0	0	0	0	0	0	1	2	2	0	0	0	0	0	1	0	0	0	0	0	1	0	0	0	1	0
CT	0	0	0	0	0	0	0	0	0	0	0	0	0	0	0	0	0	0	0	0	0	0	1	0	0	1	0	0	0	0	0	0	0	0	0
CV	0	1	0	0	0	0	0	0	0	0	0	0	0	0	0	0	0	0	0	0	0	0	0	0	0	0	0	0	0	0	0	0	0	0	0
CW	0	0	0	0	0	2	0	0	0	0	0	0	0	0	0	0	1	0	0	0	0	1	0	0	0	0	0	0	0	1	0	0	0	0	0
CX	0	0	0	0	0	0	0	1	0	1	0	0	0	0	0	0	0	0	0	0	0	0	0	1	0	0	0	0	0	0	0	0	0	0	0
HG	0	0	0	0	0	1	0	0	0	0	1	0	0	0	0	0	0	5	0	1	0	0	0	0	0	0	0	0	0	0	0	0	1	1	0
HM	0	0	0	0	1	0	0	0	0	0	0	0	1	1	0	0	1	2	0	0	0	0	0	0	0	0	0	0	0	1	0	0	0	0	0
MN	0	0	0	0	0	0	0	0	0	1	0	0	0	0	0	0	0	0	0	0	0	0	0	0	0	0	0	0	0	0	0	0	0	0	0

Table 7. Contingency Table of Calveg (Columns) versus FIA Ground Plots (Rows), with non-conifer classes collapsed into 3 Formations.

TYPE	CP	DF	DP	JP	MF	MP	PJ	PP	PR	RD	RF	RW	SG	WJ	HdWd	Shb	Hrb	Tot	% Agr
CP	0	0	0	0	0	0	0	0	0	3	0	0	0	0	0	0	1	4	0
DF	0	42	2	0	2	13	0	1	0	25	0	0	0	0	37	2	3	127	33
DP	0	2	4	1	0	16	0	0	1	0	0	0	0	0	1	2	0	27	15
GF	0	1	0	0	0	0	0	0	0	1	0	0	0	0	0	1	0	3	0
JP	0	0	0	4	10	4	0	2	0	0	1	0	0	0	3	6	0	30	13
KP	0	0	0	0	0	1	0	1	0	0	0	0	0	0	1	1	0	4	0
LP	0	0	0	0	1	1	0	0	0	0	0	0	0	0	0	0	0	2	0
MF	0	0	1	2	53	71	0	13	0	0	10	0	0	0	9	16	0	175	30
MP	0	0	0	6	17	67	0	12	0	0	2	0	0	1	10	6	0	121	55
PE	0	0	0	0	0	0	1	0	0	0	0	0	0	0	0	0	0	1	0
PJ	0	0	0	1	1	1	6	0	0	0	0	0	0	1	0	3	2	15	40
PM	0	0	0	0	0	0	0	0	0	1	0	0	0	0	0	0	0	1	0
PP	3	1	0	8	2	40	1	20	0	0	1	0	0	1	10	16	0	103	19
RD	0	4	0	0	0	0	0	0	0	100	0	0	0	0	9	6	0	119	84
RF	0	0	0	0	3	3	0	0	0	0	7	0	0	0	0	0	0	13	54
RW	0	0	0	0	0	0	0	0	0	35	0	0	0	0	15	3	0	53	0
SG	0	0	0	0	0	0	0	0	0	0	0	0	2	0	0	0	0	2	100
WF	0	0	0	0	5	3	0	1	0	0	3	0	0	0	2	2	0	16	0
WJ	6	0	0	0	1	3	0	0	0	0	0	0	0	5	1	23	1	40	13
HdWd	0	22	1	5	0	62	1	15	0	24	0	1	0	1	179	43	8	362	49
Shb	2	1	0	3	4	11	1	13	0	2	1	0	0	0	42	27	4	111	24
Hrb	0	0	0	0	1	1	0	0	0	1	1	0	1	1	9	1	2	18	11
Total	11	73	8	30	100	297	10	78	1	192	26	1	3	10	328	158	21	1347	
% Agree	0	57	50	13	53	23	60	26		52	27		66	50	55	17	10		

Agree 38.5%
Expected 12.8%
Kappa 29.4%

Table 8. Contingency table comparison of CALVEG (columns) versus FIA field data (rows), in which rows and columns have been sorted based on agglomerative cluster analysis to display similarities among types in misclassification errors. Primary clusters are indicated by horizontal and vertical lines.

	Hdwd	MP	RD	Shb	MF	DF	PP	RF	JP	Hrb	PJ	CP	WJ	DP	SG	PR	RW
Hdwd	179	62	24	43	0	22	15	0	5	8	1	0	1	1	0	0	1
RD	9	0	100	6	0	4	0	0	0	0	0	0	0	0	0	0	0
MF	9	71	0	16	53	0	13	10	2	0	0	0	0	1	0	0	0
MP	10	67	0	6	17	0	12	2	6	0	0	0	1	0	0	0	0
PP	10	40	0	16	2	1	20	1	8	0	1	3	1	0	0	0	0
DF	37	13	25	2	2	42	1	0	0	3	0	0	0	2	0	0	0
Shb	42	11	2	27	4	1	13	1	3	4	1	2	0	0	0	0	0
RW	15	0	35	3	0	0	0	0	0	0	0	0	0	0	0	0	0
WJ	1	3	0	23	1	0	0	0	0	1	0	6	5	0	0	0	0
DP	1	16	0	2	0	2	0	0	1	0	0	0	0	4	0	1	0
JP	3	4	0	6	10	0	2	1	4	0	0	0	0	0	0	0	0
Hrb	9	1	1	1	1	0	0	1	0	2	0	0	1	0	1	0	0
RF	0	3	0	0	3	0	0	7	0	0	0	0	0	0	0	0	0
WF	2	3	0	2	5	0	1	3	0	0	0	0	0	0	0	0	0
PJ	0	1	0	3	1	0	0	0	1	2	6	0	1	0	0	0	0
CP	0	0	3	0	0	0	0	0	0	1	0	0	0	0	0	0	0
SG	0	0	0	0	0	0	0	0	0	0	0	0	0	0	2	0	0
KP	1	1	0	1	0	0	1	0	0	0	0	0	0	0	0	0	0
LP	0	1	0	0	1	0	0	0	0	0	0	0	0	0	0	0	0
PE	0	0	0	0	0	0	0	0	0	0	1	0	0	0	0	0	0
GF	0	0	1	1	0	1	0	0	0	0	0	0	0	0	0	0	0

Several patterns are obvious in the sorted matrix. Classes with few field or map samples are clearly separated from those occurring more frequently, which are concentrated in the upper left hand comer of the table. Sorting of map types is based on similar errors of commission. Hardwoods are placed at one end of the matrix, with patterns least similar to the other map classes. Shrublands, however, are placed between Redwood/Douglas Fir and Mixed Conifer/Fir. Few strong patterns of comission error are obvious, except the general similarity of Hardwoods and Mixed Conifer/Pine. In other words, patterns of comission errors are relatively class-specific.

In sorting the rows to reveal patterns of omission errors, hardwoods were again placed at one end of the order and shrublands were sorted between several conifer types. Some ground classes showed very similar patterns of omission errors. Mixed Conifer/Fir, Mixed Conifer/Pine and Ponderosa pine, which occurred in adjacent rows, were frequently confused in CALVEG. (Note that these types cluster as ground classes but not as map classes. Differences between ground and map associations include the frequent occurrence of hardwood types in Mixed Conifer/Pine polygons and their absence in the Mixed Conifer/Fir polygons.) Red Fir (RF) and White Fir (WF) also showed very similar patterns of distribution among CALVEG map classes.

When CALVEG is collapsed into Conifer, Hardwood, Shrubland and Herbaceous formation types, it displays relatively high map accuracy (65%), with an expected accuracy of 47% and kappa level of 33% (Table 9).

Conifer vegetation is mapped with much higher accuracy than the other three classes, and map accuracy weighted by class frequency, as expressed in the kappa statistic, is considerably lower. One would expect these results given that the samples were from areas expected to support conifer forests.

2.4. Spatial Patterns of CALVEG Map Errors

In this section we examine possible sources of map errors in CALVEG that range from production errors, such as errors of photointerpretation, to processing errors such as line generalization and displacement during digitizing. We also consider spatial autocorrelation of errors, boundary effects and map generalization.

2.4.1. Regional differences in classification accuracy

The location of FIA field plots are coded by region and mapped in Figure 2. Patterns of agreement between CALVEG and FIA field data are displayed in Figure 3. The small scale of the figure and overlap of symbols for closely neighboring plots make it difficult to study patterns of errors in detail. However, a tendency for higher error rates in the Coast Ranges and southern Sierra Nevada is apparent, as well as the relatively high rates of agreement for the northern Coast. The 5 Forest Service regions differed systematically in their error rates, with the lowest accuracies for Regions 2 and 4 and the highest in Regions I and 3 (Table 10).

The very low accuracy of CALVEG in Region 2 is due mainly to confusion between closely related types, notably between Mixed Conifer/Fir and Mixed Conifer/Pine and between Douglas Fir/Pine and Ponderosa Pine, and between Western Juniper and Shrublands (mostly Blackbrush) (Table 11). In general, the pattern observed for CALVEG as a whole, that is of low accuracy due to confusion among ecologically related types, holds true for each of the individual regions as well.

Table 9. Contingency table of Calveg (columns) versus FIA ground plots (rows), aggregated to 4 formations.

	Conifer	Hardwood	Shrubland	Herbaceous	Total	% Agree
Conifer	664	98	87	7	856	77.6
Hardwood	132	179	43	8	362	49.4
Shrub	38	42	27	4	111	24.3
Herbaceous	6	9	1	2	18	11.1
Total	840	328	158	21	1347	
% Agree	79.0	54.6	17.1	9.5		

Agree 64.7%
Expected 47.2%
Kappa 33.3%

Table 10. Percent agreement between the CALVEG map and FIA field plots for the five regions shown in Figure 2.

Region	# Samples	# Agree	% Agree
1	414	147	36
2	372	66	18
3	283	110	39
4	88	22	25
5	195	55	28
All	1352	400	30

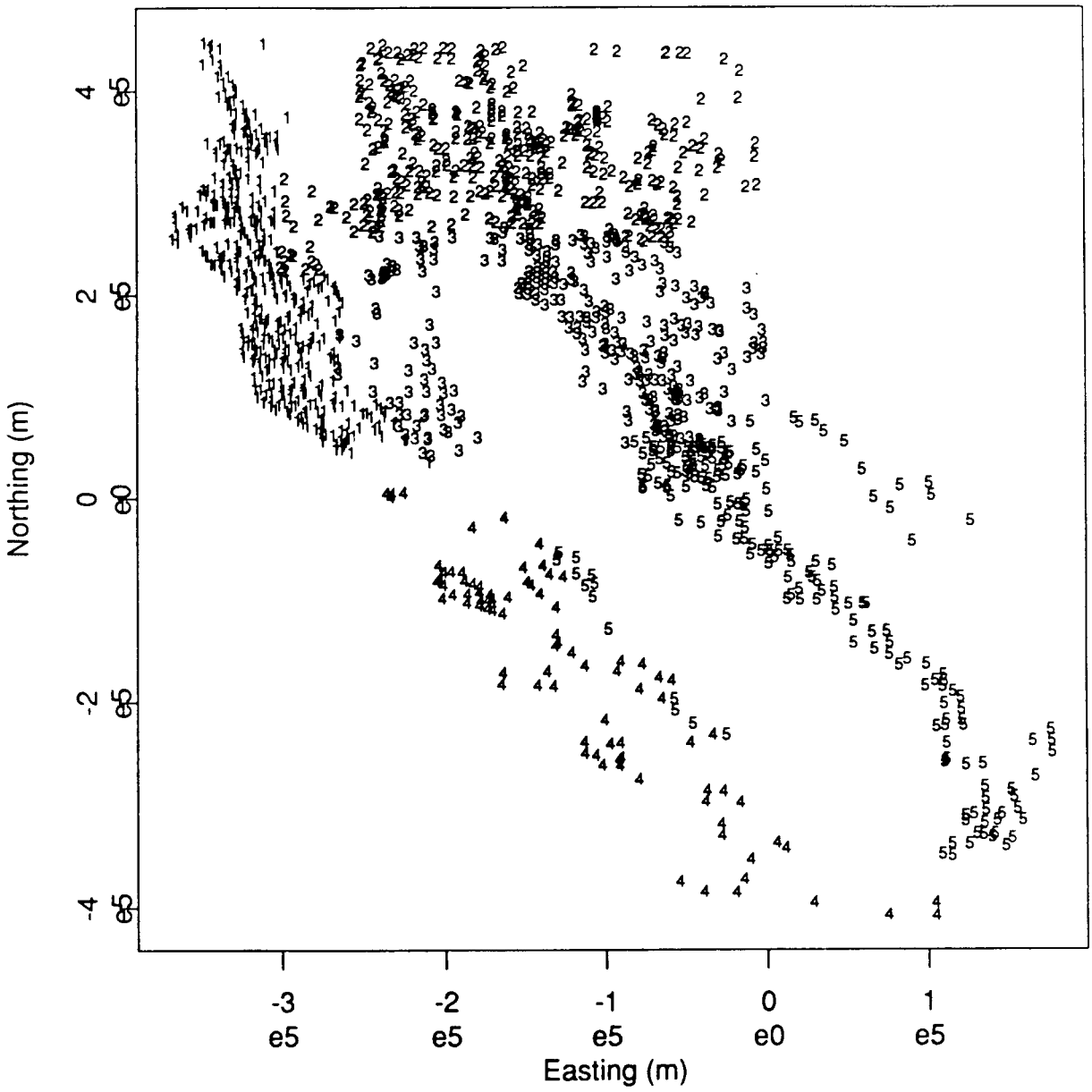

Figure 2. Map of FIA field plots with plot's labelled by region number

Figure 3. Map of FIA field plots color coded to indicate agreement (green) or disagreement (red) with the CALVEG map. Map was produced by overlay of FIA points and CALVEG polygons using ARC/INFO.

Table 11. Contingency table of CALVEG (columns) versus FIA ground plots (rows) for Region 2 (see Figure 2). Non-conifer types are collapsed into formations. See Table 5 for the code to CALVEG types.

	CALVEG MAP																	
FIELD	LP	RF	WF	MF	MP	DF	DP	JP	PP	CP	KP	WJ	PJ	Hdwd	Sh	Hb	Total	%Agree
LP	0	0	0	0	1	0	0	0	0	0	0	0	0	0	0	0	1	0
RF	0	2	0	0	2	0	0	0	0	0	0	0	0	0	0	0	4	50
WF	0	3	0	3	2	0	0	0	1	0	0	0	0	1	1	0	11	0
MF	0	5	0	15	46	0	1	2	13	0	0	0	0	5	10	0	97	15
MP	0	0	0	3	13	0	0	4	9	0	0	1	0	4	1	0	35	37
DF	0	0	0	0	5	1	2	0	0	2	0	0	0	3	0	0	13	8
DP	0	0	0	1	0	0	4	0	16	0	0	0	0	0	2	0	23	17
JP	0	0	0	1	4	0	0	0	3	0	0	0	0	3	2	0	13	0
PP	0	0	0	1	12	0	0	8	18	3	0	1	0	2	6	0	51	35
CP	0	0	0	0	0	0	0	0	0	0	0	0	0	0	0	0	0	0
KP	0	0	0	0	1	0	0	0	1	0	0	0	0	1	1	0	4	0
WJ	0	0	0	1	3	0	0	0	0	6	0	5	0	1	22	1	39	13
PJ	0	0	0	1	0	0	0	1	0	0	0	0	0	0	0	0	2	0
Hd	0	0	0	0	16	1	0	2	7	0	0	0	0	13	9	0	48	27
Sh	0	1	0	3	8	0	0	2	5	2	0	0	0	2	6	1	30	20
Hb	0	1	0	0	1	0	0	0	0	0	0	1	0	0	0	0	3	0
Total	0	12	0	29	114	2	7	19	73	13	0	8	0	35	60	2	374	

Agree 20.6%
Expected 10.6%
Kappa 11.2%

Table 12. Contiguity analysis of map classes for widespread conifer and hardwood types in the CALVEG map. Table entries are the number of shared arcs between row and column pairs. Only half of the symmetrical matrix is shown. Abbreviations for vegetation types are those in Table 5.

	DF	JP	MF	MP	PP	QG	QK	RD	RW	DP
DF	-	37	62	17	0	13	5	23	0	11
JP		-	62	25	5	5	0	3	0	5
MF			-	82	7	10	23	0	0	9
MP				-	28	15	51	0	0	6
PP					-	1	14	0	0	0
QG						-	0	0	0	5
QK							-	12	0	1
RD								-	0	0
RW									-	0
DP										-

Table 13. Parameters for the Exponential Variogram model calculated by least squares regression. Parameters were not estimated for Regions 4 or 5 because of the small sample sizes for those areas.

Region	Sill	Range (km)	Model r^2
Regions 1-5	0.213	41.1	0.64
1	0.243	132.9	0.60
2	0.147	112.0	0.41
3	0.241	10.2	0.58

2.4.2. Spatial relations of frequently confused vegetation types

A number of studies have shown that different conifer types appear very similar in Landsat MSS imagery (Hoffer et al. 1979, Strahler 1981, Yool et al. 1986, Cibula and Nyquist 1987). Thus where these types occur adjacent to one another it may not be possible to discriminate them by photointerpretation of MSS imagery. Accordingly, we hypothesized that high rates of confusion would occur during photointerpretation of conifer types occupying adjacent polygons. We tested this for the entire CALVEG. map by tabulating the frequency with which different frequently confused types shared a common arc, where an arc is a polygon boundary segment connecting two points at which the boundary has been digitized (Table 12). Arcs were of relatively uniform length in the digital CALVEG map.

Douglas Fir shared common borders, in descending frequency, with Mixed Conifer/Fir, Jeffrey Pine, Redwood/Douglas Fir and Mixed Conifer/Pine. The latter two were often confused with this class, but the Mixed Conifer/Fir was not a source of mapping error for this class. Mixed Conifer/Fir, which was most often confused with Mixed Conifer/Pine, also shared many common arcs with that type. Thus there is mixed evidence for confusion of spatially contiguous conifer types.

2.4.3. Spatial autocorrelation of vegetation classification errors

In addition to broad regional differences in map accuracy, there is evidence that errors were non-randomly distributed within regions. We used the variogram, which is based on geostatistical theory, to test for spatial dependence in misclassification of field plots by CALVEG. A brief description of this method that has been summarized from Dubayah et al. (1990) is provided below.

Each plot was coded as 0 or I depending on whether it was incorrectly or correctly classified. We assumed that the resulting binary variable could be described by a random variable, F (x) where x was a position vector. Assume that this variable is second-order stationary with a mean, m, then for all x:

$$\mathrm{var}[F(\mathbf{x})] = E\{[F(\mathbf{x}) - m]^2\} = C(0) \tag{3}$$

$$\gamma(\mathbf{h}) = \frac{1}{2} E\{[F(\mathbf{x}+\mathbf{h}) - F(\mathbf{x})]^2\} = C(0) - C(\mathbf{h}) \tag{4}$$

The quantity, C (0), the covariance at zero lag, is simply the variance of the spatial process and is called the a priori variance. The semi-variance, $\gamma(h)$, is equal to the variance minus the covariance at lag h. The lag h is a vector quantity having both a direction and magnitude. If the semi-variance is isotropic, then h reduces to a scalar.

The essential features of the semi-variogram are the sill, the range, and the "nugget variance". By definition the semi-variance at zero lag must be zero, but experimental semivariograms, when extrapolated to the ordinant, may have some positive intercept value known as the nugget variance. The semi-variance can increase monotonically from this point to a maximum value called the sill. The sill, if it exists, is the a priori variance of the data.

The lag at which the sill is reached is called the range and represents the distance to which the data are spatially dependent or autocorrelated. There is no finite range if the sill is approached asymptotically. The semi-variance may also increase indefinitely with lag. In this case the process is not second-order stationary since it has no finite variance (i.e. the a priori variance does not exist).

Anisotropic (directional) and isotropic semi-variograms were calculated for the entire sample and for each of the four forest regions based on all possible inter-plot distances. There was no evidence of directional differences in the variograms, so only the isotropic analyses are presented here. Even though the semi-variograms were calculated over the full range of distances, we limited our analysis to a spatial lag of 100 km. To provide consistent estimates of the sill and range of the variograms, each was then fitted to a variety of parametric curves using a least squares criterion (Caceci and Cacheris 1984). An exponential of the form:

$$\gamma(h) = C(1 - e^{-h/r}) \tag{5}$$

provided the best fit to the data. In this equation, C is the sill or a priori variance, and r a distance parameter related to the range. Since the sill is reached asymptotically in the exponential model, the range is not definite. However, other researchers have defined a working distance of a = 3r at which point the variance is approximately 95% of the sill value (Oliver and Webster, 1986).

Variograms for the entire study area and for study regions 1-3 are shown in Figure 4. For the full data set and for Regions 1-3, there is evidence of fairly strong autocorrelation in classification accuracy of neighboring locations (1-2 krn separation), especially in Regions 1 and 3. All regions exhibit increasing semi-variance at longer lag distances. This "drift" in the variogram, which is greatest for Region 2, indicates trends or pattern at larger scales that is due to regional differences in average error rates. Because of this drift, the exponential models do not fit the data closely (Table 13). Although the fitted models give estimates of the range of spatial dependence from 10 to 132 km, visual inspection of the variograms indicates that local autocorrelation is important up to distances of 3-5 km.

The variograms capture some of the basic patterns in errors that are apparent in Figure 3, that is the combination of local clustering as well as regional patterns in average error rates. The high local autocorrelation means that FIA plots cannot be treated as independent samples. To the extent that one observation can be predicted from its immediate neighbors, the effective sample size is considerably less than the number of plots. This will affect estimates of sample variance and will thus also undermine the use of significance tests for comparing error rates among types or regions.

The local autocorrelation in errors could be due to a number of factors, including the concentration of errors near polygon boundaries, misclassification of polygons containing several field samples, high rates of agreement or disagreement for specific environments or vegetation types, etc. Several analyses were conducted to help identify the probable causes of nonrandom error distribution, as described in the following sections.

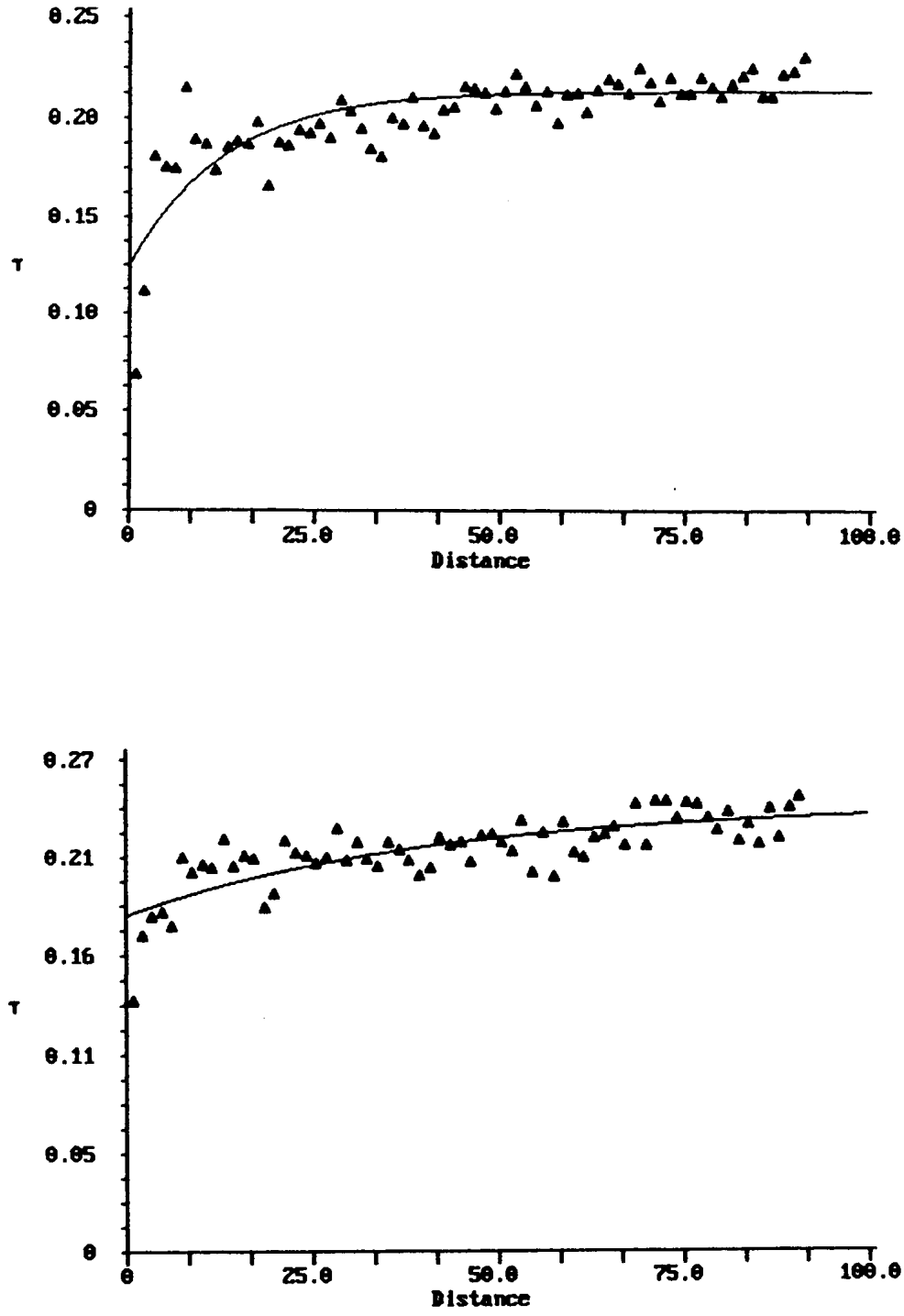

Figure 4. Variogram showing semivariance of map errors in CALVEG (based on comparison with FIA field data) as a function of lag distance (km) for all regions (top) and for Region 1 (bottom).

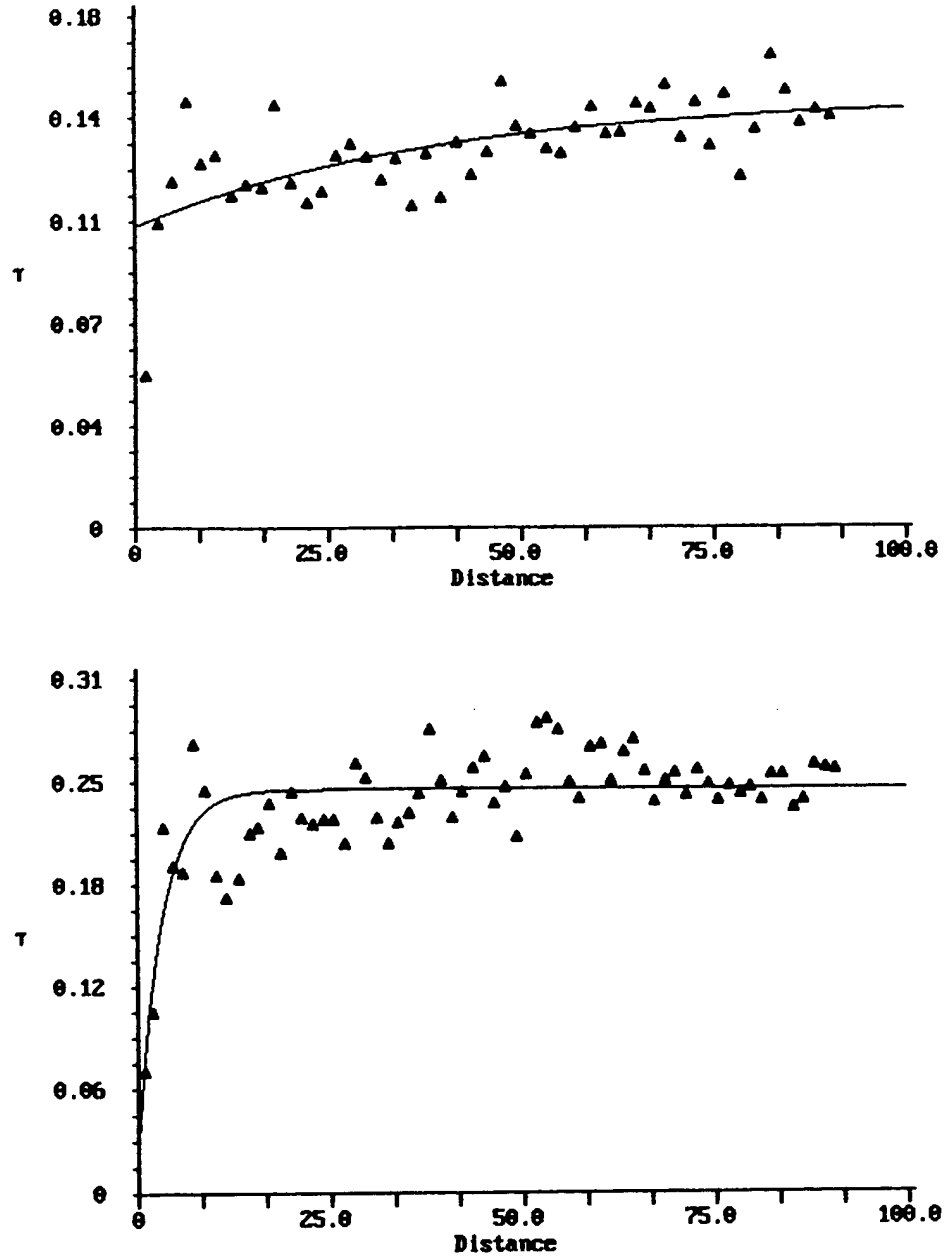

Figure 4. Variogram showing semivariance of map errors in CALVEG (based on comparison with FIA field data) as a function of lag distance (km) for Region 2 (top) and for Region 3 (bottom).

2.4.4. Distribution of errors with respect to polygon boundaries

Vegetation frequently exhibits compositional gradients rather Um abrupt transitions from one type to the next, making it difficult to delineate polygon boundaries. Also, when vegetation types do not exhibit strong spectral contrast, polygon boundaries cannot be placed between adjacent types with much reliability. If one or both of these conditions apply, one would predict that map efforts should increase near polygon boundaries. On the other hand, if types are separated by sharp boundaries and/or are spectrally contrasting, one might expect map errors to be lower near polygon boundaries, and higher at the interior of polygons, where errors of map generalization might be more frequent.

We tested for these effects by comparing the distances to the nearest arc for correctly and incorrectly classified field plots. Incorrectly classified plots were significantly closer to polygon boundaries than correctly classified plots, although the difference in average distance was not great and there was a lot of scatter in the data (Figure 5). This pattern was generally true for individual conifer types as well (Figure 6). With the exception of Ponderosa Pine, misclassified plots were closer to polygon boundaries than correctly classified plots. However, only the Recwood/Douglas Fir type showed a significant boundary effect.

2.4.5. Polygon digitizing errors

Error is introduced into digital maps during line digitizing due to scanning and registration errors for maps produced by digital scanners, or by line generalization, displacement and registration errors for maps produced by manual digitizing. We assessed digitizing error for the portion of the CALVEG map covering the southern Sierra Nevada, delineated by a I degree block of the eastern half of the United States Geological Survey (USGS) 1:250,000 scale Bakersfield quadrangle map (Figure 7). This test site, hereafter referred to as the Bakersfield site, is characterized by a complex mix of conifer forest and woodland of several dominant species, several oak communities, and various shrub and herbaceous vegetation. The site spans the Sierra Nevada range from the intensively developed agricultural region of California's San Joaquin Valley to the west, to the Mojave Desert, consisting primarily of creosote bush and Joshua tree communities in the east.

The magnitude of digitizing error was estimated using two versions of the Bakersfield map. One version, from CDF's GIS database, had been scan digitized from the original mylars, mosaiced into a single statewide coverage, and then smoothed with a spline function. We also manually digitized the mylar of the Bakersfield site twice to permit comparison of data input methods and of two different human digitizers (M. Painho and D. Stoms). All versions were transformed into UTM projection.

To compare lines from the different digital maps, six thousand vertices on a manually digitized version were selected, and then the shortest distances to boundaries on the other versions were computed by the GIS. The distances were not signed, so magnitudes but not directions were determined.

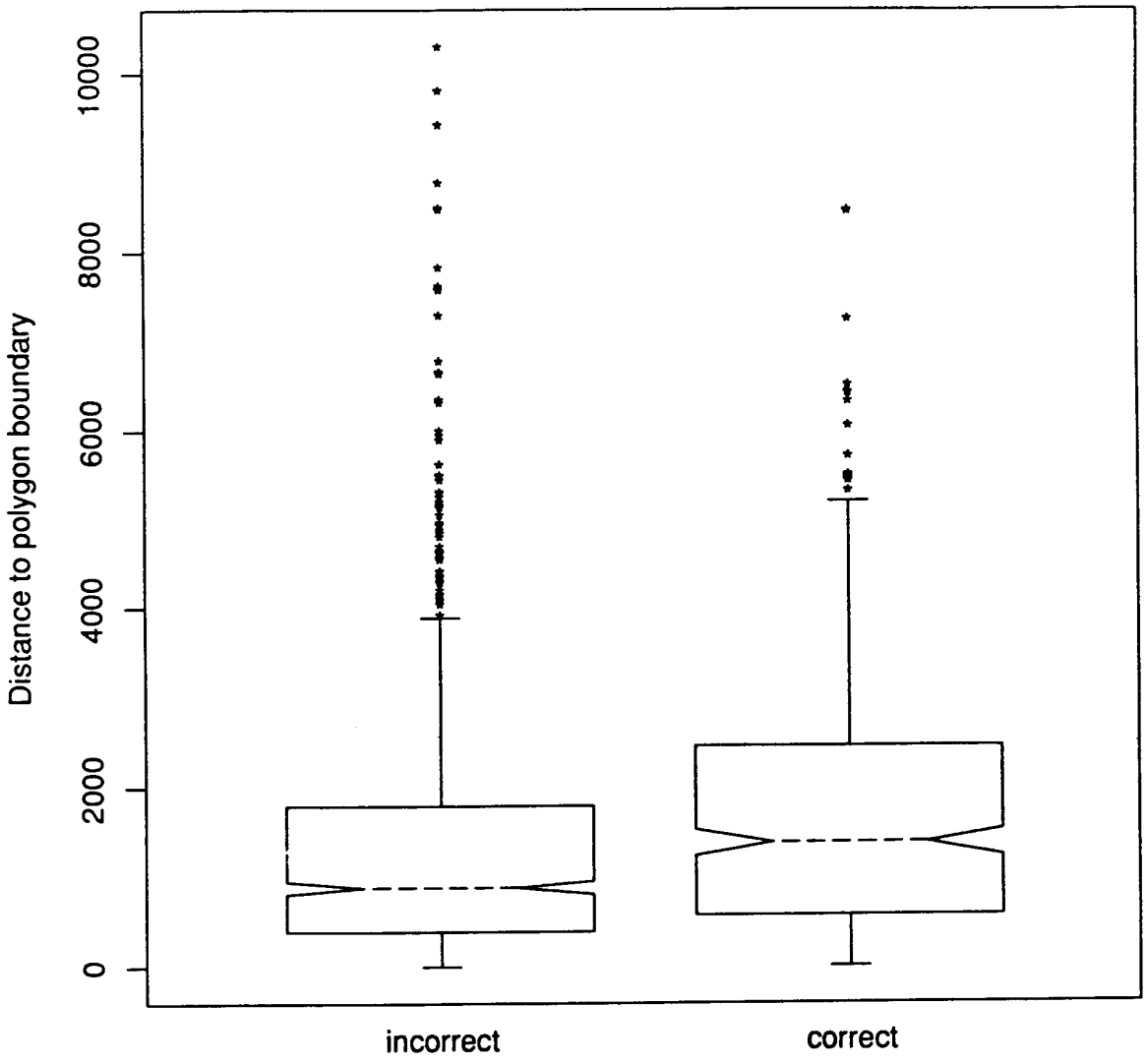

Figure 5. Boxplots showing the frequency distribution of distance from a field plot to the nearest polygon boundary in the CALVEG map, for incorrectly versus correctly classified plots. Horizontal lines of the boxes indicate median and quartile values. Vertical lines span the range of the data, excluding outliers (asterisks). Non-overlapping of notches indicates significant difference of the means at $p < 0.05$.

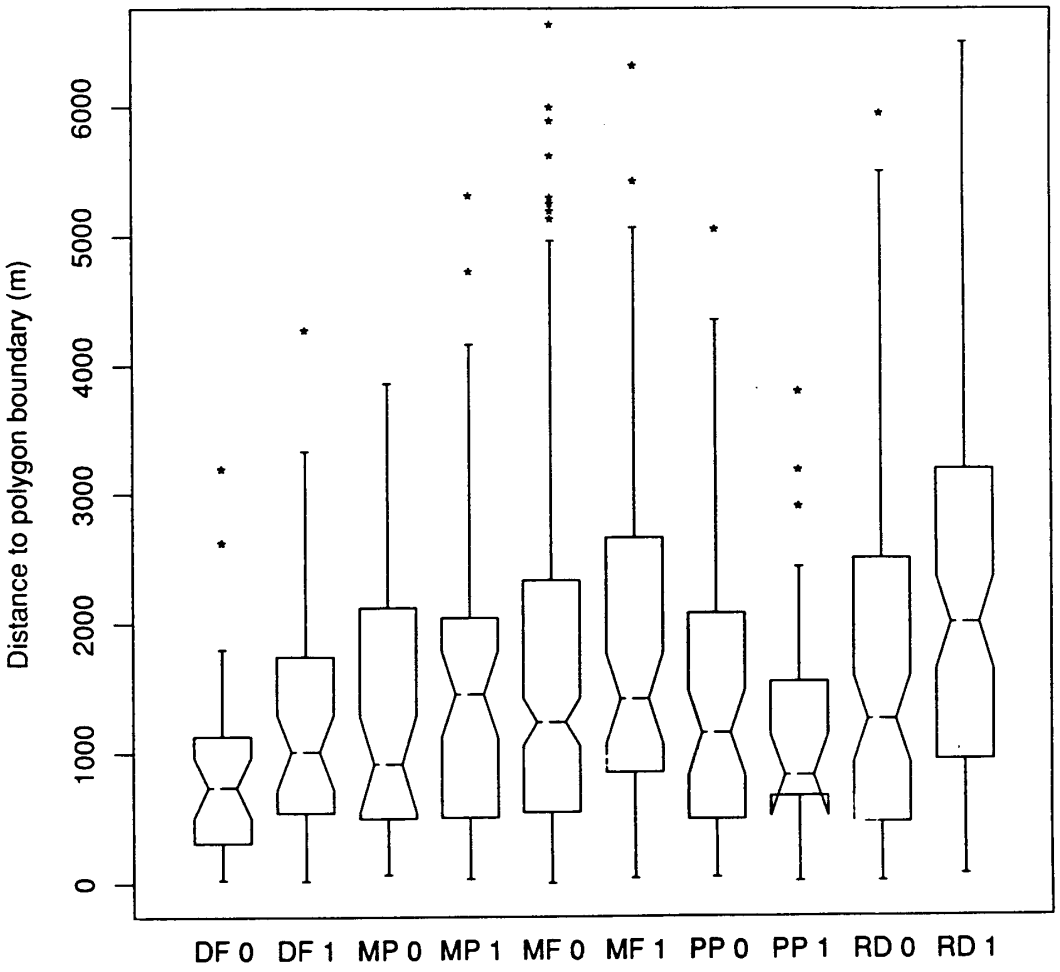

Figure 6. Boxplots showing the frequency distribution of distance from a field plot to the nearest polygon boundary in CALVEG for selected Conifer types, for incorrectly (0) versus correctly (1) classified plots. See Figure 5 for an explanation of boxplots. Types include Douglas Fir (DF), Mixed Conifer/Pine (MP), Mixed Conifer/Fir (MF), Ponderosa Pine (PP) and Redwood/Douglas Fir (RD).

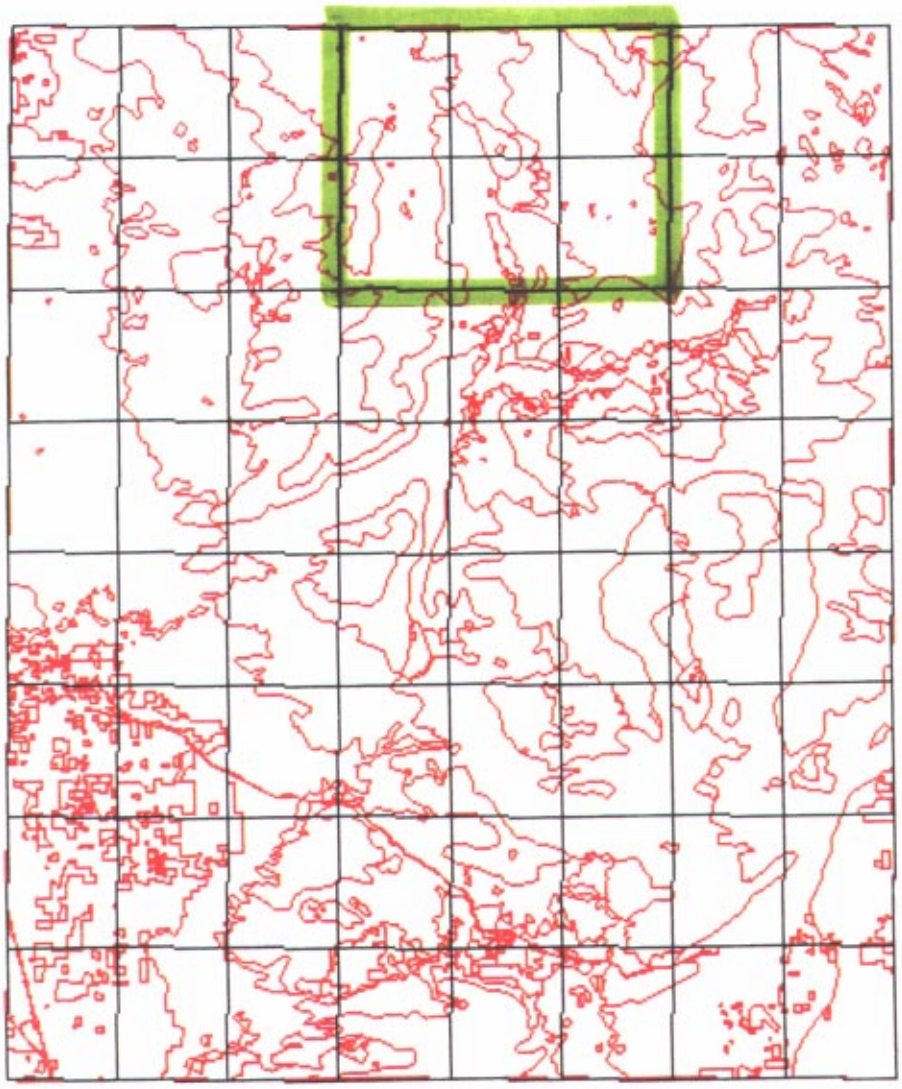

Figure 7. Portion of the CALVEG map occupying the eastern half of the U.S. Geological Survey 1:250,000 Bakersfield quadrangle. The area is 1 by 1 degree (roughly 10,000 sq. km). The grid indicates the boundaries of 64 U.S.G.S. 7.5 minute quadrangles. The heavy line at the northern edge of the region encloses six 7.5 minute quadrangles covering a portion of the Sequoia National Forest, in which CALVEG was compared to U.S. Forest Service Timber Survey maps.

A histogram of separation distances between lines that were digitized by the two analysts is shown in Figure 8. The distances are normally distributed, with 90% of the offsets less than 108 in, and 95% less than 130 in. These ground distances correspond to 0.42 and 0.52 min displacement on the manuscript map. The offsets from the scanned CALVEG map (that had also been smoothed with a spline function) are much larger than between the two manually digitized versions (Figure 9). The offsets between CDF&FP's version and the manually digitized versions were also normally distributed but with much larger standard deviations. 90% of the offsets were less than 252 in and 95% were less than 292 in, corresponding to 1.00 mm and 1. 17 mm displacements on the manuscript map. In visually comparing the scanned map to those produced by manual digitizing, there appeared to be a somewhat systematic offset that we suspect was caused be problems in registration and projection transformations. In any event, given the relatively large size of most CALVEG polygons, displacements of less than 250 in probably do not account for much of the observed high error rate. The main source of disagreement between the map and field data appears due to map generalization, as discussed below.

2.5. Generalization as a Source of Map Error

Map generalization is the simplification of observable spatial variation to allow its representation on a map. 'Me Minimum Mapping Unit is intended to establish the level of generalization in interpretation of imagery, but it is rarely applied consistently across map classes or regions. Generalization also applies to the simplification of map boundaries during digitizing. Measures of map accuracy do not explicitly consider generalization effects, although excessive line generalization and spatial filtering can greatly reduce the predictive value of a map. We have used photointerpreted transects and larger scale vegetation maps to study generalization effects on the accuracy of CALVEG. The transect data were also used to study the positional accuracy of polygon boundaries.

2.5.1. Transect analysis of map generalization and boundary location

A total of one hundred 4000 meter transects were analyzed within the Bakersfield test site. Initially, a large number of random points were located within the boundaries of the study area in the east half of the USGS 1:250,000 Bakersfield quad. Next the CALVEG map was recoded into conifer and non-conifer areas. (This was to eliminate any uncertainty in photointerpretation of cover type along the transects). By overlaying the simplified CALVEG map and the random points two new sets of random points were obtained: (1) points within the boundaries of conifer lands and (2) points outside conifer lands. 50 points in each map class (100 total) were randomly chosen for the analysis. The distance between the random points and the closest conifer boundary were calculated in the GIS. 50 points (25 from each set) closest to a conifer boundary were repositioned on that boundary. This resulted in three subsets of points:

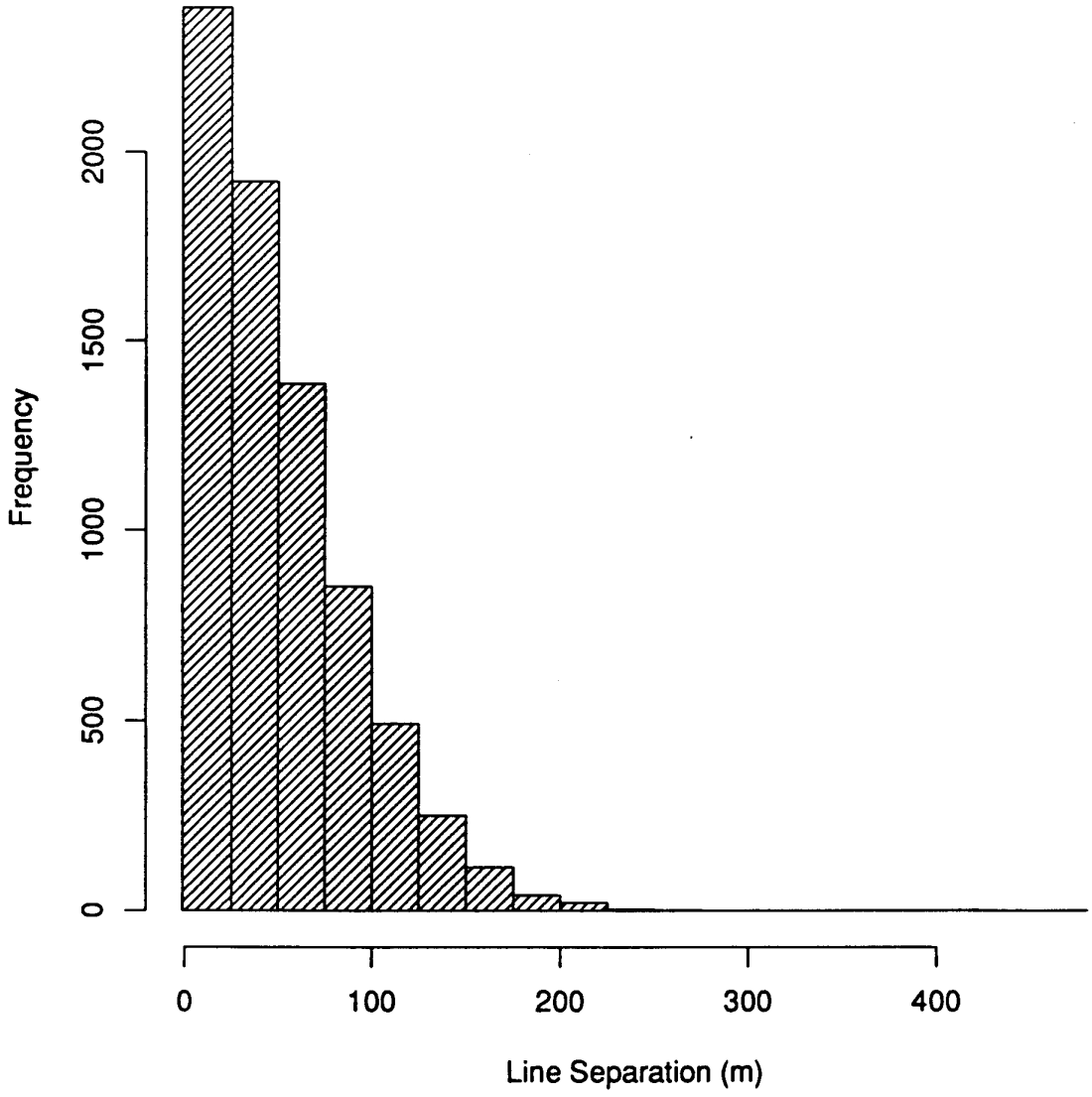

Figure 8. Frequency distribution of separation distances between the same CALVEG polygon boundaries that were digitized by two analysts.

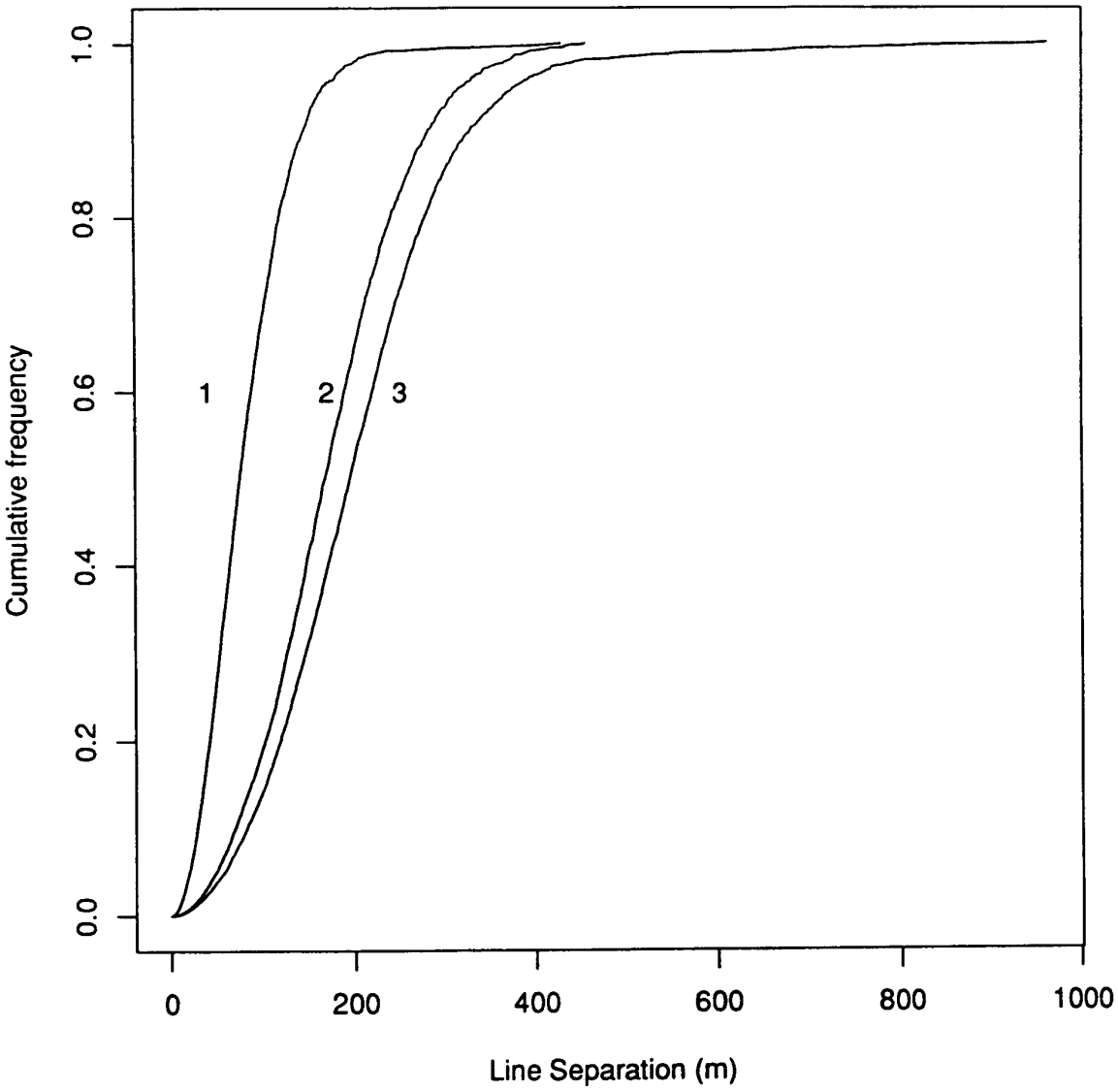

Figure 9. Cumulative frequency distribution of displacement distances between the same CALVEG polygon boundaries for maps manually digitized by Marco Painho versus David Stoms(1), and for CDF's scanned digital product versus maps manually digitized by David Stoms (2) and Marco Painho (3).

1) 25 points in CALVEG conifer polygons;

2) 25 points in non-conifer polygons;

3) 50 points on conifer polygon boundaries.

The transects were obtained by generating a 4000 meter line centered on the random points. In order to account for terrain orientation, transects were alternately ordered northsouth and east-west. The transects were divided into 500 m intervals, plotted on transparency paper at the 1:62,500 scale and manually overlain on 15-minute U.S.G.S. quads. Vegetation along the transects was mapped using 1987, 1:58,000 NHAP color infrared photography. The transects were interpreted for land cover in 500 meter intervals, using a simplified classification scheme derived from CALVEG and shown in Table 14. A zoom transfer scope was used to adjust the scale of the photography and the plots containing the transects. Although some locational error was unavoidable, registration of photos to the base map was certainly accurate to within I mm on the map, or 63 m on the ground, This source of error was minor in testing CALVEG in 500 m block sizes.

The accuracy of the CALVEG map along the transects was first computed with an overall accuracy index (Table 14). In this case the length of the transects was used instead of cell counts, for a total of 200 500 m segments. Only transects not centered on CALVEG boundaries were used. A kappa statistic was also computed according to Rosenfield and Fitzpatrick-Lins (1986). The percent agreement was 40% and kappa was 26.39%. These values are very low considering the large spatial scale and the simple vegetation classification scheme.

We hypothesized that because the 500 m (equivalent to 25 ha) interval was still below the nominal MMU of CALVEG, the errors could be due to map generalization. To test this hypothesis, 4 moving windows of sizes 500, 1500, 2500 and, 4000 meters were passed along the transects and the percent correct and incorrect computed. The transects not centered on conifer boundaries were divided in two sets: (1) transects contained inside conifer polygons as defined in CALVEG (14 transects) and, (2) transects contained in non conifer polygons (I I transects). For conifer polygons, the results show a slight increase in agreement with longer windows (Figure 10), suggesting that smaller windows depict detail not mapped in CALVEG.

Contrary to our expectations, map accuracy was not very sensitive to sampling scale. In non-conifer polygons, there is actually a slight decrease in agreement with increased window size (Figure 11). This indicates that map errors for these types in this region are primarily due to polygon misclassification.

In a related analysis of map generalization, transects located in conifer forest and conifer woodland polygons were aggregated in 500, 1000 and 2000 meter blocks. Figures 15 shows the distribution of vegetation types along the transects contained in conifer forest and conifer woodland polygons. The transects located in conifer forest were correct for all segment lengths 44% of the time. The main confusion was with the conifer woodland and herbaceous types. ne transects located in conifer woodland were correct 33 percent of the time.

Table 14. Contingency table comparison of CALVEG (rows) with vegetation observed along 25 8 km transects (columns). GIS overlay of transect data and the CALVEG map were used to calculate total meters in each combination of map and ground class.

	PHOTO TRANSECT									
CALVEG	CF	BF	CW	BW	Sh	DS	Hb	Ag	Total	% Agree
CF	16219	500	4500	4170	2000	0	500	0	27890	58.2
BF	0	0	1552	0	111	0	1500	122	3285	0
CW	12430	0	5455	501	6934	0	1000	0	26320	20.1
BW	1500	0	948	5199	1889	0	3846	378	13759	37.8
SW	0	0	0	0	0	0	3417	0	3417	0
Sh	354	0	1000	2237	9500	0	4235	0	17326	54.8
Hb	0	0	0	2502	0	1495	3500	16	7512	46.6
Ag	0	0	0	0	0	0	0	484	484	100
	30504	500	13455	14610	20434	1495	17988	1000	99994	

Agreement 40357/99994 m
% Correct 40.36
% Expected 18.97
Kappa Level 26.39

Legend

Ag Agriculture/Urban	CF Conifer Forest	Hb Herbaceous
BF Broadleaf Forest	CW Conifer Woodland	Sh Shrubland
BW Broadleaf Woodland	DS Dwarf Shrubland	SW Succulent Woodland

Table 15. Contingency table comparison of CALVEG (rows) with FIA photo plot data (columns) for the Bakersfield test site.

	FIA PHOTO DATA									
CALVEG	CF	BF/BW	CW	Shb	Hb	Ba	Wa	Ag	Total	%Agree
CF	27	31	0	15	0	1	0	2	76	36
BF/BW	21	541	11	158	9	1	1	10	752	72
CW	5	101	211	110	0	0	0	3	430	49
SW	0	1	2	3	1	0	0	0	7	0
Sh	4	177	71	74	1	1	1	2	331	22
Hb	0	20	0	35	3	0	1	2	61	5
Ag	0	4	1	2	2	1	1	6	17	35
Total	57	875	296	397	16	4	4	25	1674	

Agree 53.5%
Expected 33.0
Kappa 27.7

Legend

CF Conifer Forest	SW Succulent Woodland	Ba Barren
BF Broadleaf Forest	Sh Shrubland	Wa Water
CW Conifer Woodland	DS Dwarf Shrubland	Ag Agriculture/Urban
BW Broadleaf Woodland	Hb Herbaceous	

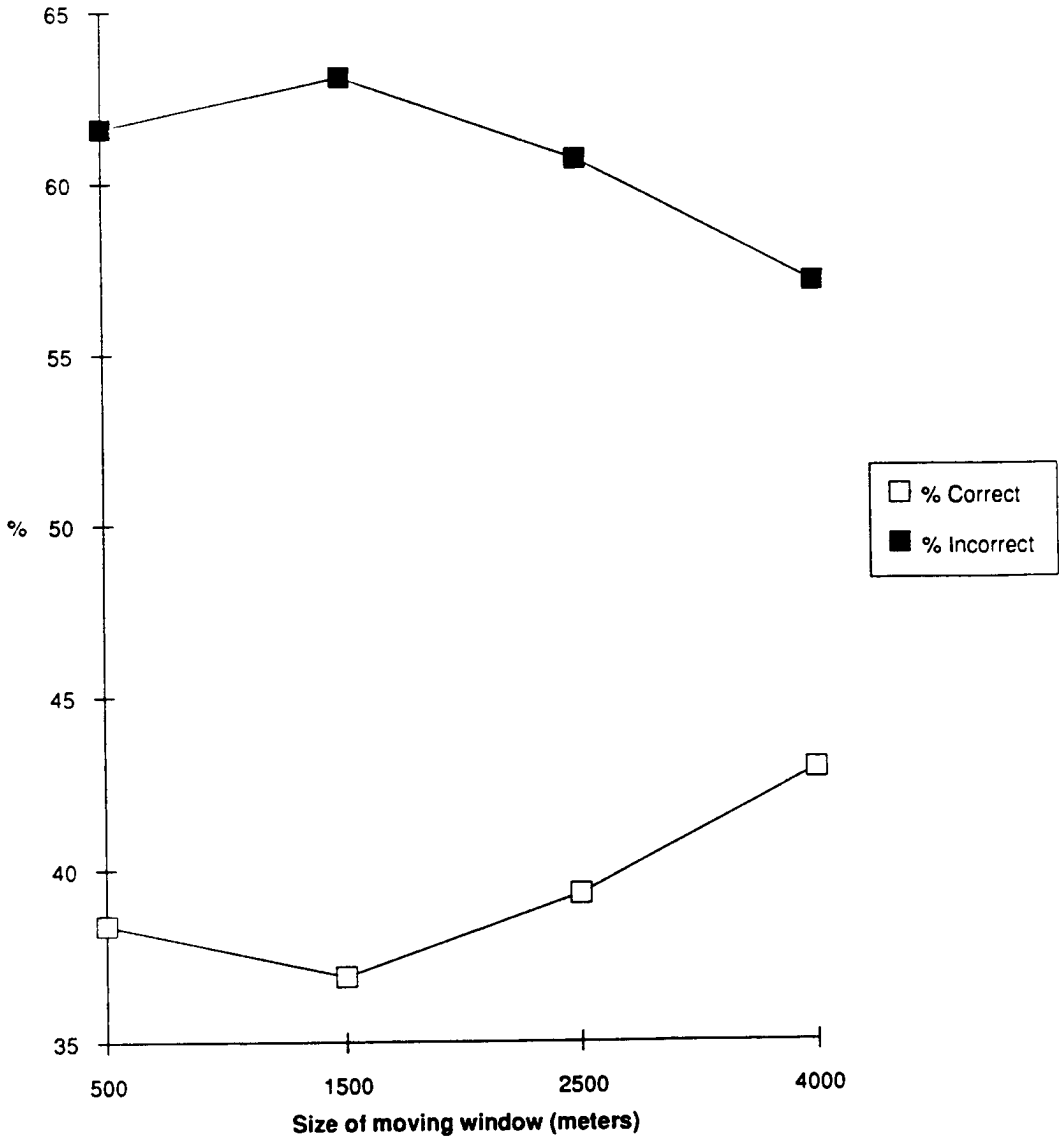

Figure 10. Percent agreement between areas mapped in CALVEG as Conifer-dominated vegetation and 1986 vegetation cover photointerpreted along fourteen 4 km transects, as a function of the length of transect used for the comparison.

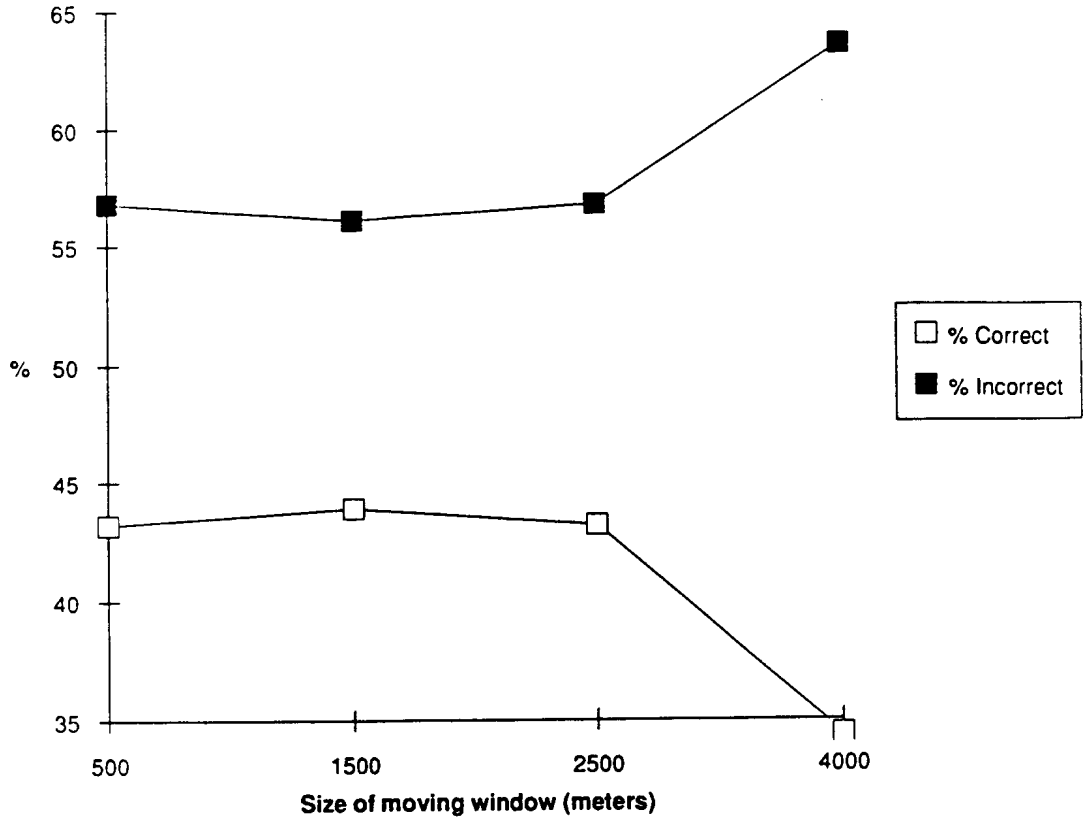

Figure 11. Percent agreement between areas mapped in CALVEG as non-Conifer vegetation and 1986 vegetation cover photointerpreted along fourteen 4 km transects, as a function of the length of transect used for the comparison.

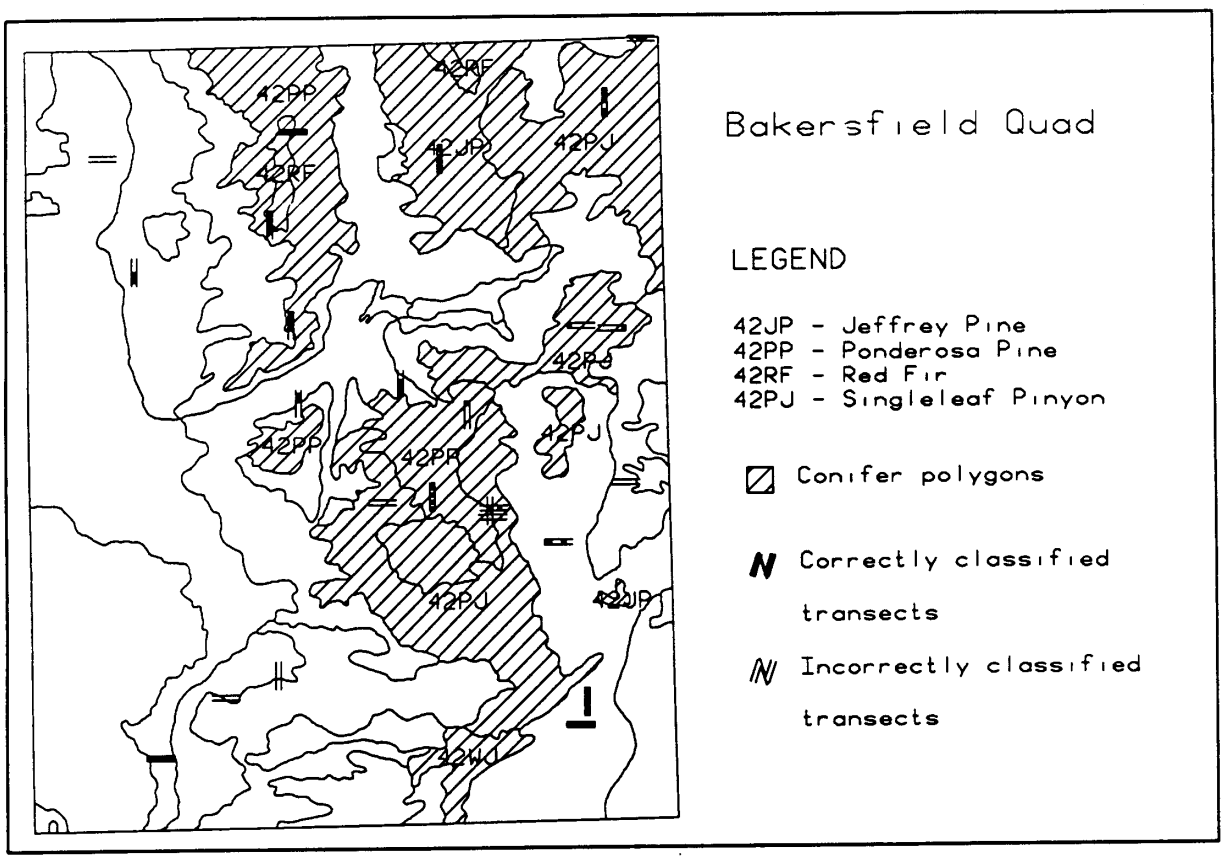

Figure 12. Map showing 4 km transects superimposed on the CALVEG polygons for the Bakersfield test site. Solid shading indicates 500 m transect segments that agree with the map at the simple level of conifer versus non-conifer types.

Here the main confusion was with conifer forest which, according to the transects, is as common as conifer woodland. There is also some confusion with the shrub class.

The spatial distribution of the correctly and incorrectly classified transects discussed above can also be observed in Figure 12, which compares CALVEG to 1674 FIA photo plots for the test sites. There is generally low agreement between the photoplots and the CALVEG map (Table 15). The values computed were respectively 25.99% for overall percent correct and 12.36% for the kappa statistic. The CALVEG classes with highest disagreement are conifer woodland and broadleaf woodland (both confused with broadleaf forest and shrub), and shrub (confused with broadleaf forest). Conversion of the FIA vegetation classification system to CALVEG may have accounted for some of the errors, but the main problem seems to be polygon misclassification rather than generalization error. Most of the correctly mapped photoplots were located on broadleaf forest polygons at the south/center of the map and also on conifer woodlands in the northeast. The incorrectly classified photo plots were mostly located on broadleaf woodland on the west part of the map and also, on conifer woodland in the south/center.

We should note that the high density of FIA data for private, forested areas of the state provides an opportunity to recode those portions of the CALVEG map where polygon labels disagree with photoplot data. However, the much simpler classification scheme used in the FIA survey and the sparse coverage over non-forested regions and public lands means that this can provide only piecemeal editing of CALVEG at the formation or sub-formation level of classification.

2.5.2. Comparison of CALVEG with larger scale map data

Large scale vegetation data were obtained from 1:24,000 scale timber inventory maps supplied by the Sequoia National Forest. These maps were derived from photo interpretation of 1:24,000 1976 aerial photography. Therefore, the dates of the imagery on which the vegetation maps are based are comparable. The vegetation classes on the large scale maps differ from the CALVEG system in that commercial conifer classes are delineated with greater detail, distinguishing by size class and tree density as well as dominant species. Hardwoods, shrubs, and other land cover types are generally not further subdivided by species or vegetation structure. Thus, whereas the conifer types can be aggregated into CALVEG classes, the other types are not as detailed as CALVEG. One map sheet was digitized for comparison with the small scale map, but was mainly used to extract random sample points with their vegetation classifications.

One dataset of ground truth was a sample of 42 timber inventory plots made by the Sequoia National Forest staff in 1988. The plots, all in the Bakersfield quadrangle, had been selected by the Forest Service as a stratified random sample of the commercial timber strata on the National Forest. Thus, these points emphasize the conifer cover types, although one plot turned out to be all hardwoods and four were mixed stands of hardwoods and conifers. Records for each plot consisted of their UTM coordinates to the nearest 100 meters and the diameter breast height (dbh) for every tree in the plot. We translated each plot record into a corresponding class of the CALVEG system.

The contingency tables are presented in Tables 16 through 18. In Table 16, the 42 timber inventory plots made in 1988 are compared to the 1980 CALVEG map. Individual class accuracy was very low for the CALVEG map classes, with no class greater than 25 percent agreement. Overall agreement was a meager 19 percent; Kappa at only 0.08 was close to a random assignment to classes; and accuracy was only 5.7 percent at the 95 percent confidence level. By far the biggest source of disagreement was the assignment of many plots to a Mixed Conifer/Fir class which did not even occur on the map of the Bakersfield site. Mixed Conifer-Fir in CALVEG is a transitional class containing a combination of Fir and pine species that separately dominate the adjacent purer classes. Thus, much of the disagreement occurs between taxonomically (in the CALVEG hierarchical system) and ecologically similar classes and is not as poor as might at first appear. Note also that three plots occurred in Canyon live oak stands, even though they were chosen to sample conifer stands on the timber inventory currently being developed for the Sequoia National Forest (Bob Rogers, personal communication). Thus, these three samples also are in conflict with new, large scale mapping.

The substantial disagreement between small scale mapping and very large scale plots could be explained by two main factors. One explanation would state that the plots and map units are simply too mismatched in spatial resolution and that for a small sample of 42 plots, one could expect poor agreement as the plots sample the within-class heterogeneity. In other words, the plots may be the wrong tool to assess accuracy on small scale maps. As noted earlier, differences in sample scale could also confound tests of CALVEG using FIA ground and photo plots. At the very least, comparison of CALVEG with relatively small plots provides information about within-polygon heterogeneity. With agreement rates well below 40%, one must conclude that, at best, CALVEG is over-generalized.

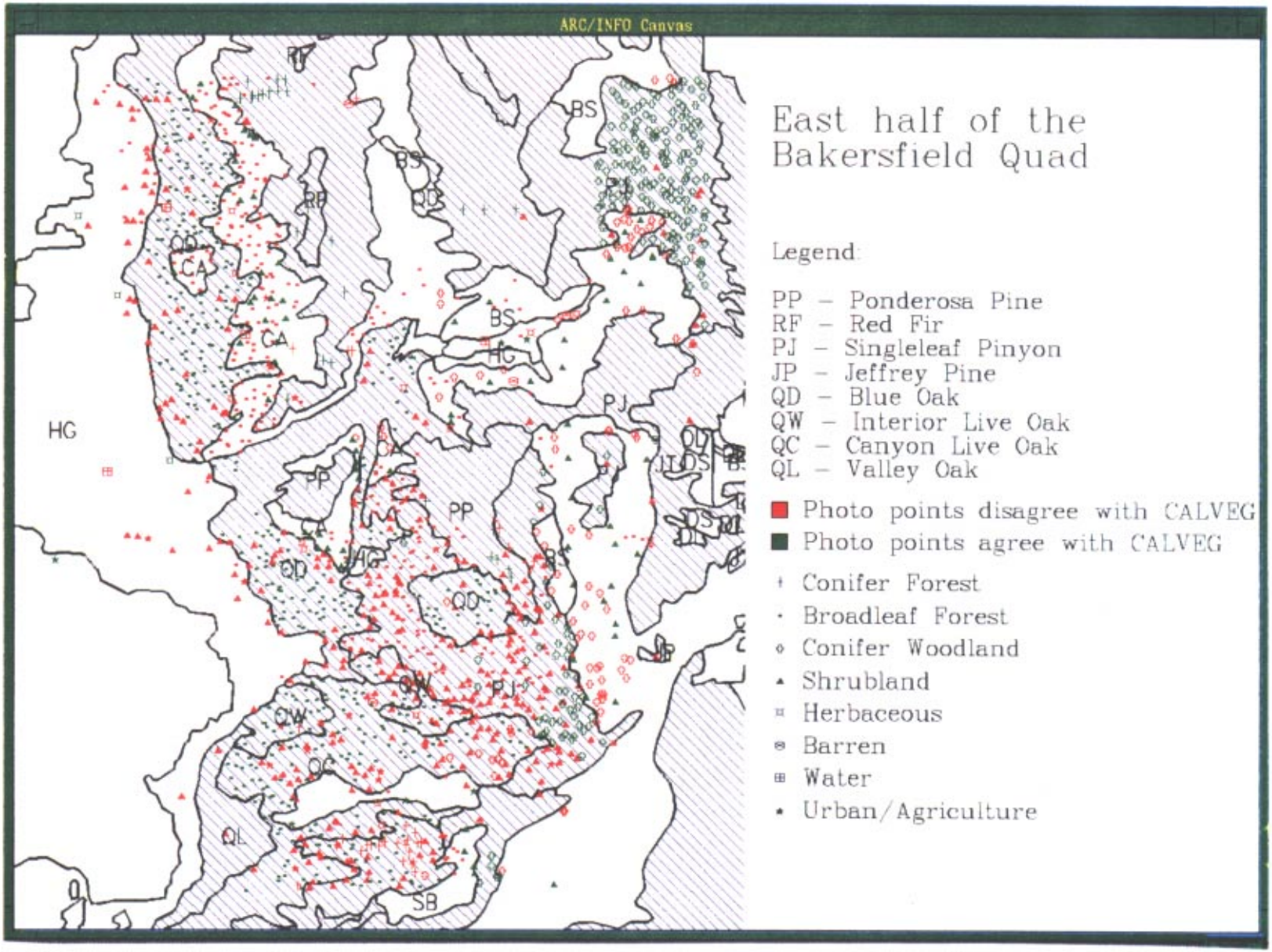

Figure 13. Overlay of FIA photo plot data on the CALVEG map for the Bakersfield test quadrangle.

A second possible explanation is that the plots accurately portray the vegetation pattern and that either the map units are mislabeled or that boundaries are badly placed. To test for such effects, we compared the CALVEG map with large scale 1980 timber inventory maps. These 1:24,000 scale maps reflect a greater degree of heterogeneity, perhaps more accurately characterizing the complexity of the vegetation mosaic. Further, the large scale map units integrate a wider area in the interpretation than the plot data. Therefore, it is assumed that the resolution is more appropriate for comparison with CALVEG.

Table 17 shows the resulting contingency table for 429 random points in the Bakersfield site. Originally, 500 random pairs of coordinates were generated, but 71 of these fell on boundaries between map units or were unlabeled, and therefore were discarded. The remaining data provided us a much larger sample to work with than the field plots.

There are some differences in structure of this table from the previous one. In the timber inventory maps, Jeffrey and Ponderosa Pine are not distinguished, so these CALVEG classes have been combined in the table. Likewise, hardwoods, shrubs, and herbaceous patches are aggregated into three broad categories as they are on the 1:24,000 scale maps.

The level of overall agreement is considerably higher than in Table 16, although still only a modest 42 percent. The Ponderosa/Jeffrey pine class shows similar agreement to the overall level at 39 percent. Interestingly, the consumer's accuracy (i.e., the column percentages) indicates a fairly good agreement (86 percent) for points on the timber inventory maps that are labeled as Ponderosa Pine. The difference between 39 percent and 86 percent means that most of the errors are of the commission type, with few omissions. Furthermore, the omission errors, as seen in Figure 14, all occur just outside the pine units on the CALVEG map, so that a slight boundary adjustment would improve the level of agreement.

The commission errors for Ponderosa Pine appear to be of two types. The first type is similar to that of Table 17, with many large scale map units labeled as a mixed conifer class. However, 36 observations of Ponderosa Pine on CALVEG were hardwood, 52 were shrub, and 3 were herbaceous on the large scale maps. This broad mix of types reflects the degree of heterogeneity within a single CALVEG map unit in a complex landscape mosaic of meadows, riparian corridors, oak stands, brush fields, and clearcuts. This heterogeneity is especially apparent in the overlay of timber inventory map classes on CALVEG. A wide range of vegetation types are mapped at the 1:24,000 scale that are enclosed within single CALVEG polygons.

Clustering of timber inventory types suggests that meaningful vegetation pattern could be mapped at the 1:250,000 scale, but that CALVEG polygons are both too generalized and poorly placed to capture this pattern. Red Fir shows poor agreement in both the rows and columns, suggesting it may not be an appropriate class within the Bakersfield site.

After observing the change in agreement by changing the extent of the area of each sample, we compared the field plots and the timber inventory maps. The disturbing results of this comparison, shown in Table 18, indicate only 32% agreement between U.S. Forest Service field plots and timber inventory maps.

Table 16. Contingency table comparison of timber inventory plots made in 1988 to the 1980 CALVEG map. Abbreviations are those in Table 5.

	Timber Inventory Plots								
CALVEG	PP	RF	JP	MF	WF	MC	QC	Total	% Agree
PP	2	1	1	9	0	0	1	14	14.3
RF	0	2	0	4	1	1	0	8	25.0
JP	0	3	4	11	0	0	2	20	20.0
MF	0	0	0	0	0	0	0	0	0
WF	0	0	0	0	0	0	0	0	0
MC	0	0	0	0	0	0	0	0	0
QC	0	0	0	0	0	0	0	0	0
Total	2	6	5	24	1	1	3	42	

Overall accuracy: 8/42=19.0%
Estimated Kappa: 0.08
Lower bound for 95% confidence: 5.71%

Table 17. Contingency table comparison of 1980 Timber Map class versus Calveg map class for 429 random locations in the Bakersfield test site. See Table 10 for a key to the abbreviations of vegetation types.

	Forest Service Timber Type											
CALVEG	PP	RF	PJ	MF	WF	MC	LP	Hdwd	Shrb	Hrb	Total	% Agree
PP/JP	105	10	1	52	3	2	4	36	52	3	268	39
RF	7	1	0	10	3	0	0	3	0	0	24	4
PJ	6	0	0	0	0	0	0	0	2	0	8	0
MF	0	0	0	0	0	0	0	0	0	0		
WF	0	0	0	0	0	0	0	0	0	0		
MC	0	0	0	0	0	0	0	0	0	0		
LP	0	0	0	0	0	0	0	0	0	0		
Hdwd	0	0	1	0	0	0	0	3	10	0	14	21
Shrb	4	0	5	0	0	0	0	29	73	6	115	63
Hrb	0	0	0	0	0	0	0	0	0	0		
Total	122	11	7	62	6	2	4	71	137	9	429	
% Agree	86	9	0	0	0	0	0	4	53	0		

% Agree 42.4
Kappa 21.0

Table 18. Contingency table comparison of 1988 Timber Survey field plots versus 1980 Forest Service Timber Type maps for the Bakersfield test site.

	Forest Service Plot Type									
Timber Map	PP	RF	MF	WF	MC	LP	Hdwd	Hrb	Total	% Agree
PP/JP	5	1	12	0	0	0	2	0	20	25
RF	0	1	1	0	0	0	0	0	2	50
MF	0	2	4	0	0	0	0	0	6	67
WF	1	0	1	1	0	0	0	0	3	33
MC	0	0	1	0	0	0	0	0	1	0
LP	0	2	1	0	0	0	0	0	3	0
Hdwd	0	0	0	0	1	0	1	0	2	50
Hrb	0	0	1	0	0	0	0	0	1	0
Total	6	6	21	1	1	0	3	0	38	
% Agree	83	17	19	100	0		33			

% Agree 32.0
Est. Kappa 16.0

2.6. Use of Ancillary Data to Improve CALVEG Map Accuracy

There is a large literature on the relationship between the distribution of California plant communities and environmental variables such as geology, topography, climate and soils. For example, topographic moisture diagrams have been developed for vegetation types in the Sierra Nevada and Transverse Ranges (Vankat 1982, Borchert and Hibbard 1984). We tested the use of environmental data for refining small scale maps of frequently confused conifer types using polychotomous logistic regression models (Ezcuffa and Montana 1984). These take the form:

$$\ln \frac{P_k}{1 - P_k} = \beta_0 + \beta_1 X_1 + \ldots B_n X_n, \qquad (6)$$

where Pk is the probability of a sample belonging to vegetation type k, 0,, is a regression coefficient and X. is an independent environmental variable or interaction variable.

We tested the use of elevation, latitude and precipitation as predictors of vegetation for frequently confused conifer types including Mixed Conifer/Fir, Mixed Conifer/Pine and Ponderosa Pine using FIA field plots. We also tested for environmental association of CALVEG confusion errors among these types by comparing the environmental characteristics of correctly versus incorrectly mapped FIA plots.

None of the environmental factors or combination of factors served as a significant discriminator of frequently confused conifer vegetation types (For this reason we have not included logit regression parameters). The lack of environmental separation of these types is illustrated in Figures 14 and 15. Based on the FIA field plots, there is no clear separation of Mixed Conifer/Fir, Mixed Conifer/Pine and Ponderosa Pine by latitude and elevation (Figure 14). There is some separation of Ponderosa Pine from Mixed Conifer/Fir as a function of combined elevation and precipitation, but the relationship is not strong (Figure 15).

A slightly different question is whether errors in mapping conifer types differed systematically by environment. For example, if areas in Mixed Conifer/Fir that were misclassified as Mixed Conifer/Pine tended to occur at relatively high elevations, one latitude, precipitation, slope angle or aspect. Figure 16 shows the distribution of FIA plots that were classified as Mixed Conifer/Pine with respect to elevation and latitude. There is some separation of Ponderosa Pine from Mixed Conifer/Fir plots as a function of elevation, however, Mixed Conifer/Pine plots are distributed fairly evenly through the distribution of both of the other types. In polygons mapped as Mixed Conifer/Fir, plots in Mixed Conifer/Pine And Mixed Conifer/Fir show no separation (Figure 17). Similar results were obtained for Ponderosa Pine (Figure 18). In short, simple environmental models appear to offer no hope for improving the existing CALVEG map.

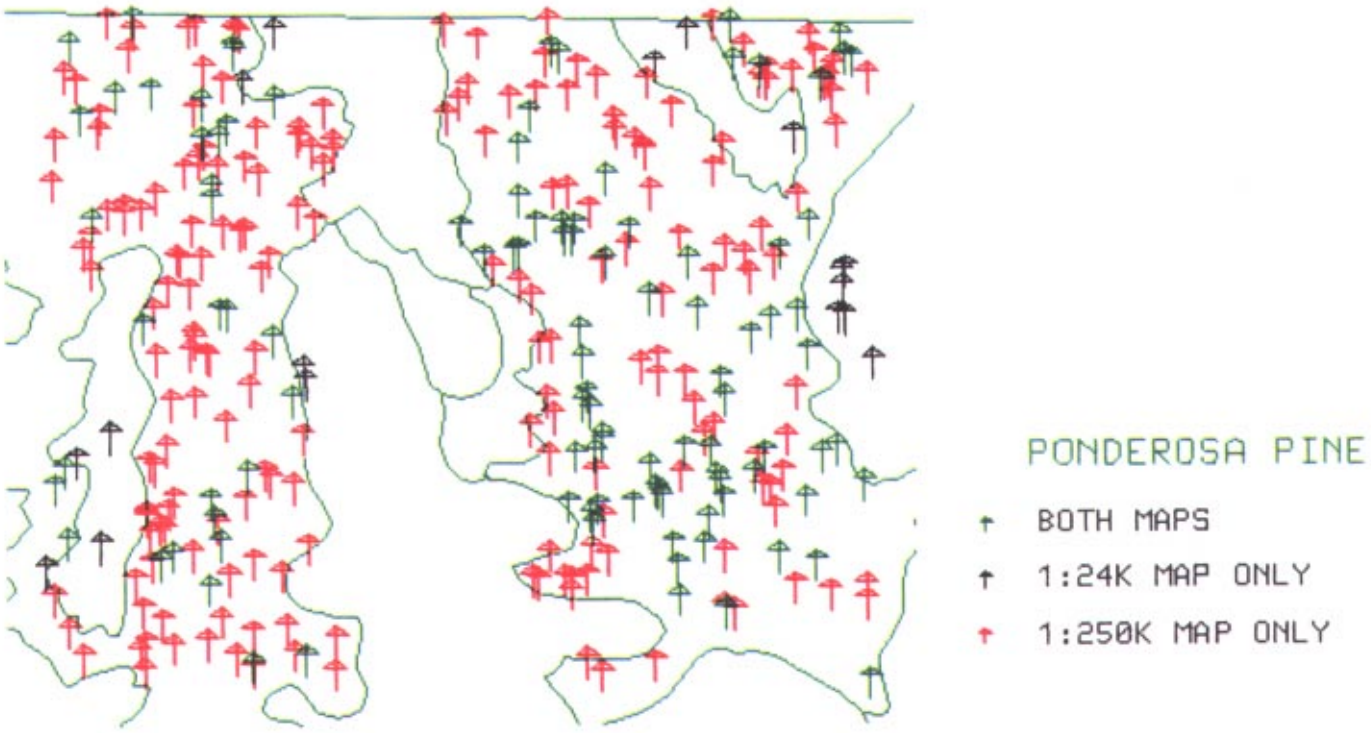

Figure 14. Overlay of CALVEG with samples from 1:24,000 U.S. Forest Service timber inventory maps, showing the location of Ponderosa Pine/Jeffrey Pine polygons in one or both maps.

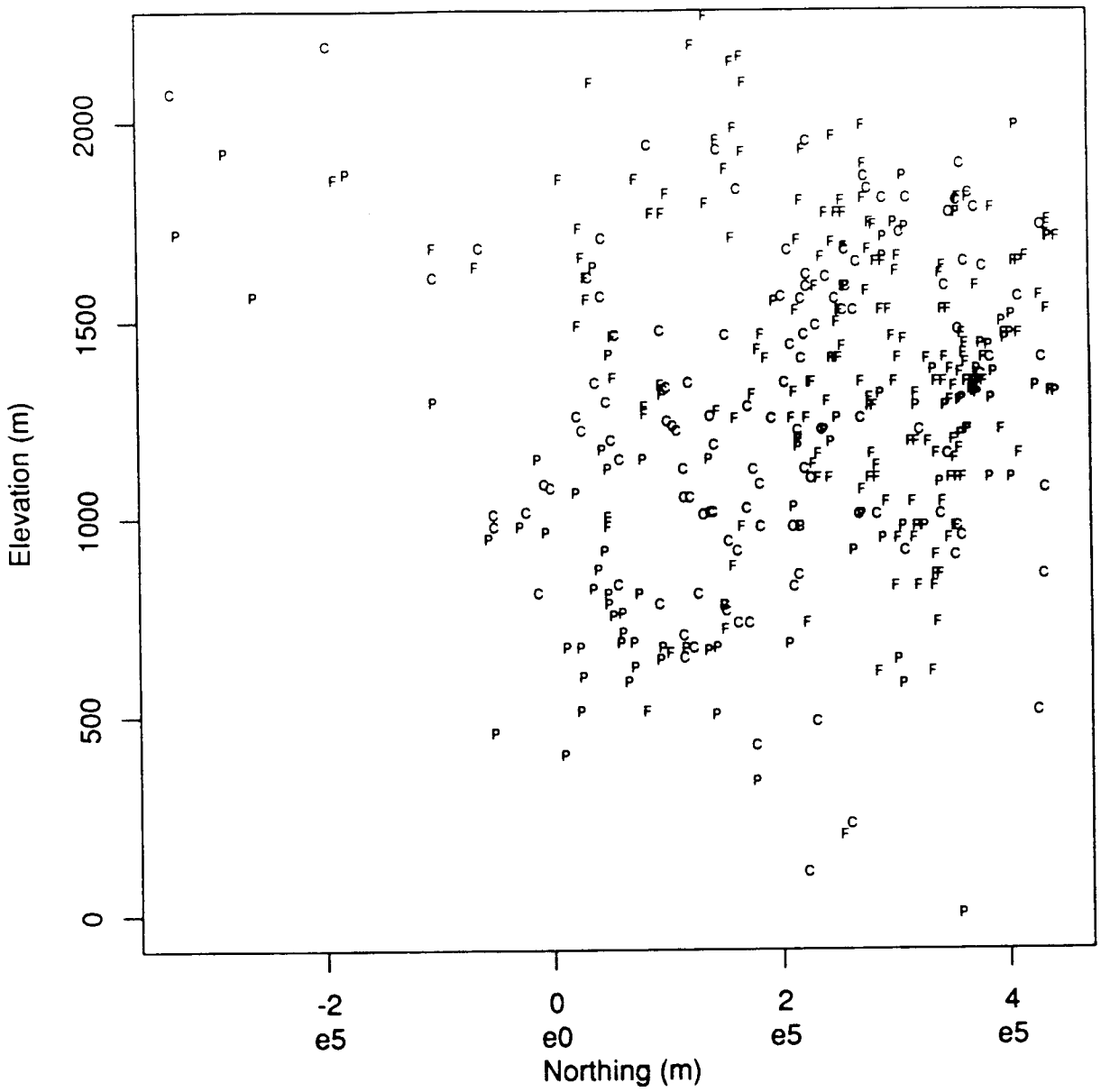

Figure 15. Scatterplot of FIA field plots as a function of latitude (UTM northing) and elevation. Symbols for the vegetation types are as follows: C - Mixed Conifer/Pine, P - Ponderosa Pine, F - Mixed Conifer/Fir.

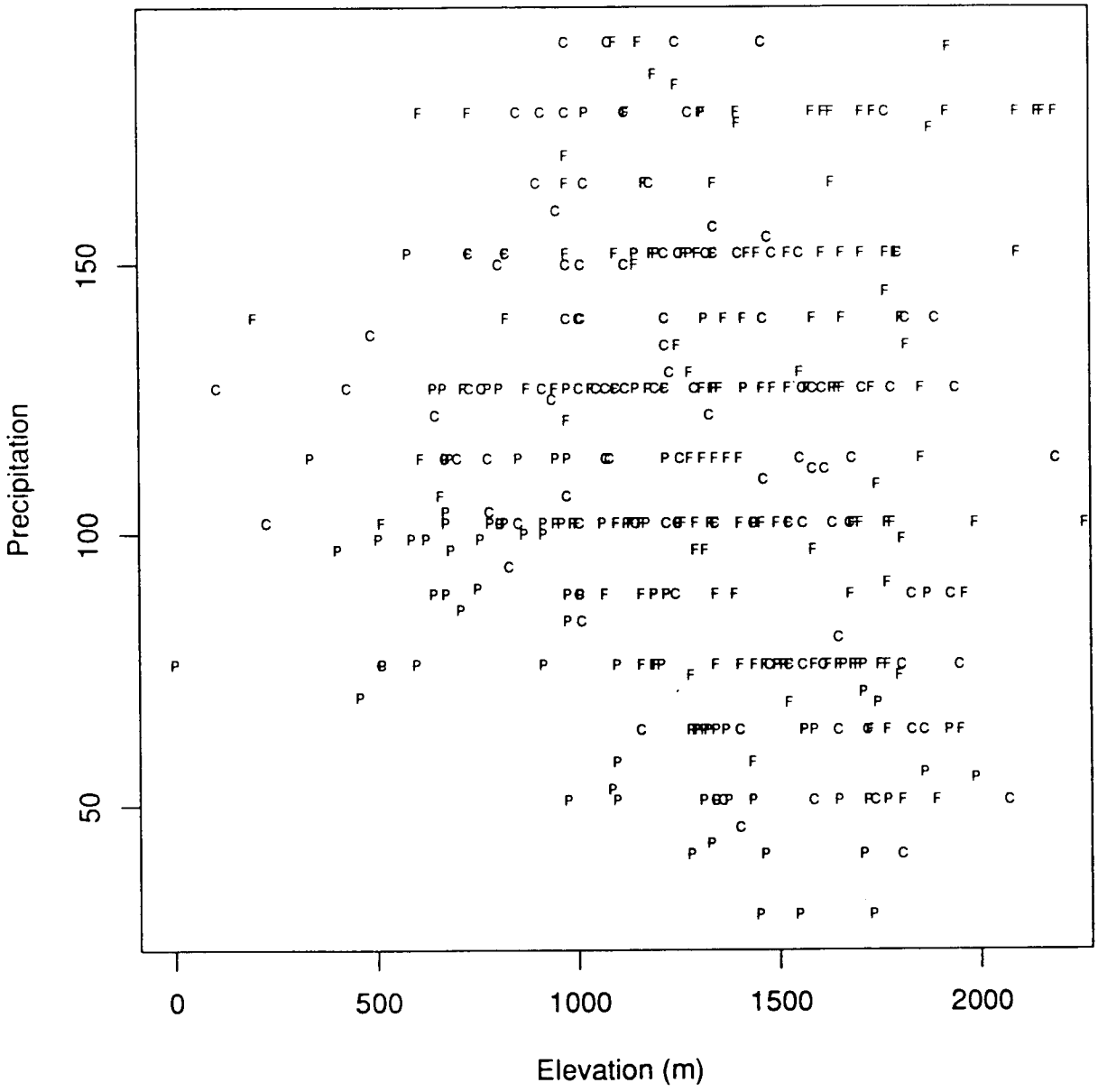

Figure 16. Scatterplot of FIA field plots as a function of elevation and precipitation. Symbols for the vegetation types are as follows: C - Mixed Conifer/Pine, P - Ponderosa Pine, F - Mixed Conifer/Fir.

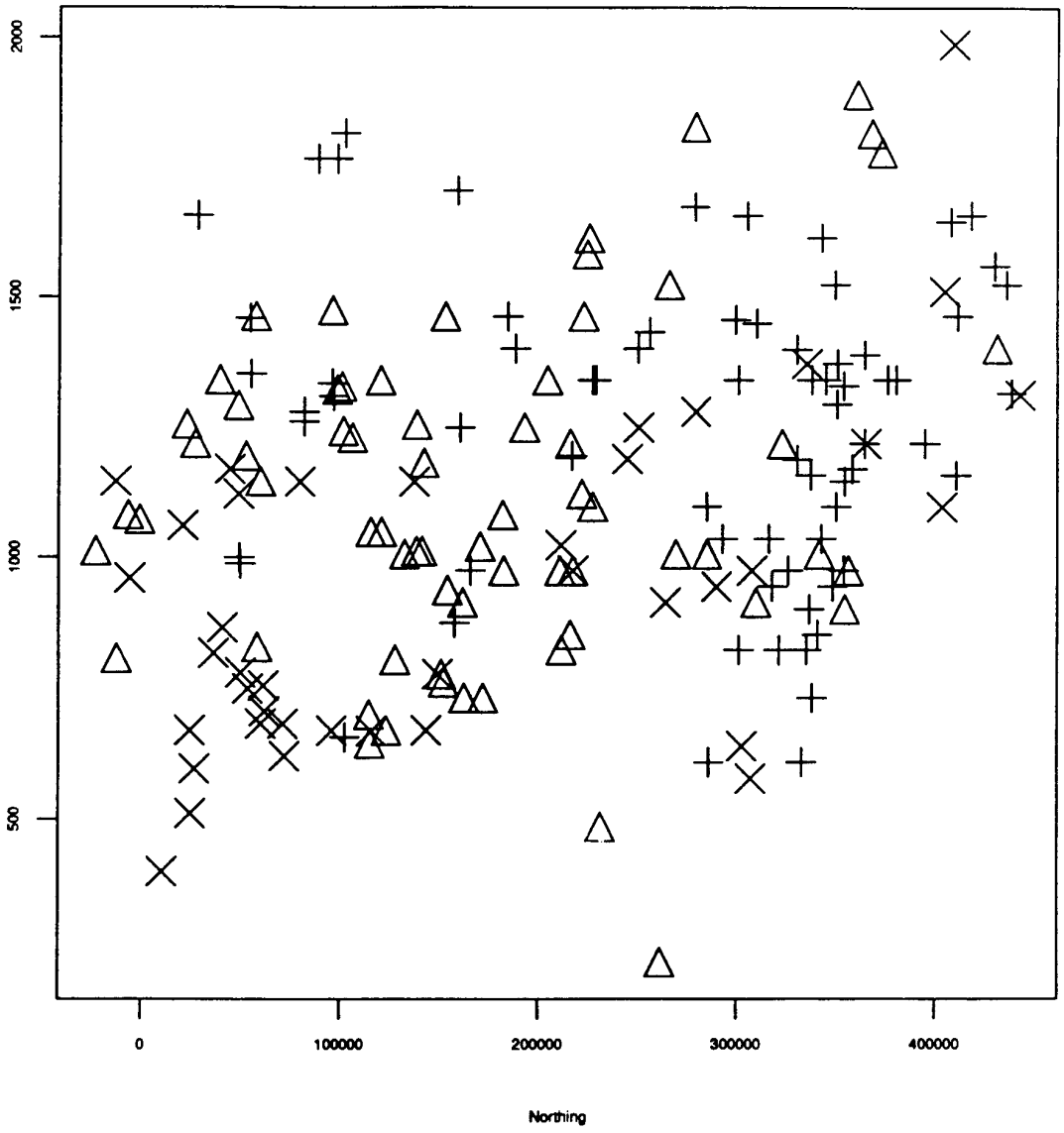

Figure 17. Scatterplot of FIA field plots as a function of latitude and elevation for CALVEG polygons in theMixed Conifer/Pine type. Symbols for the vegetation types are as follows: triangles - Mixed Conifer/Pine, X - Ponderosa Pine, + - Mixed Conifer/Fir.

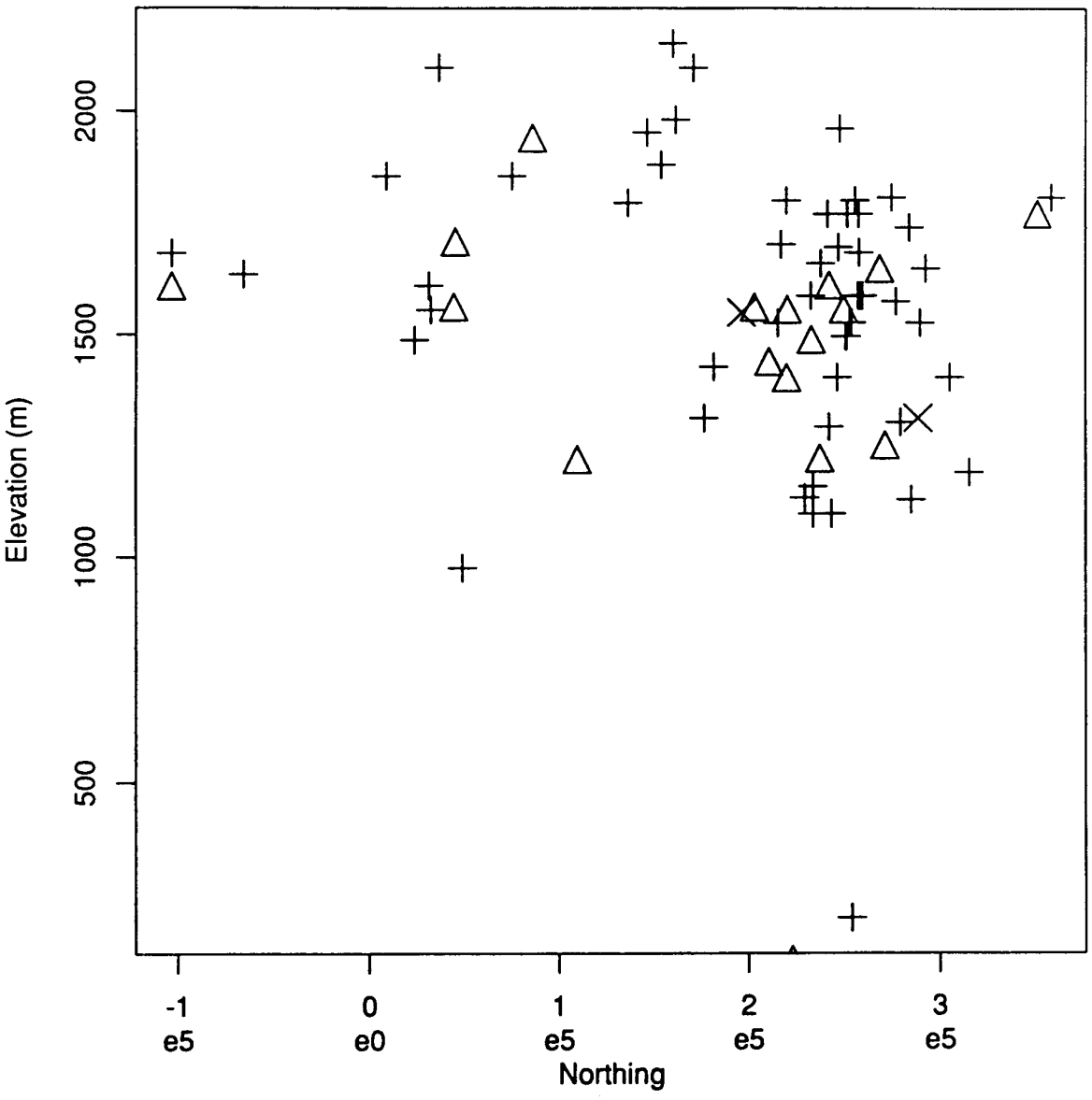

Figure 18. Scatterplot of FIA field plots as a function of latitude and elevation for CALVEG polygons in the Mixed Conifer/Fir type. Symbols for the vegetation types are as follows: triangles - Mixed Conifer/Pine, X - Ponderosa Pine, + - Mixed Conifer/Fir.

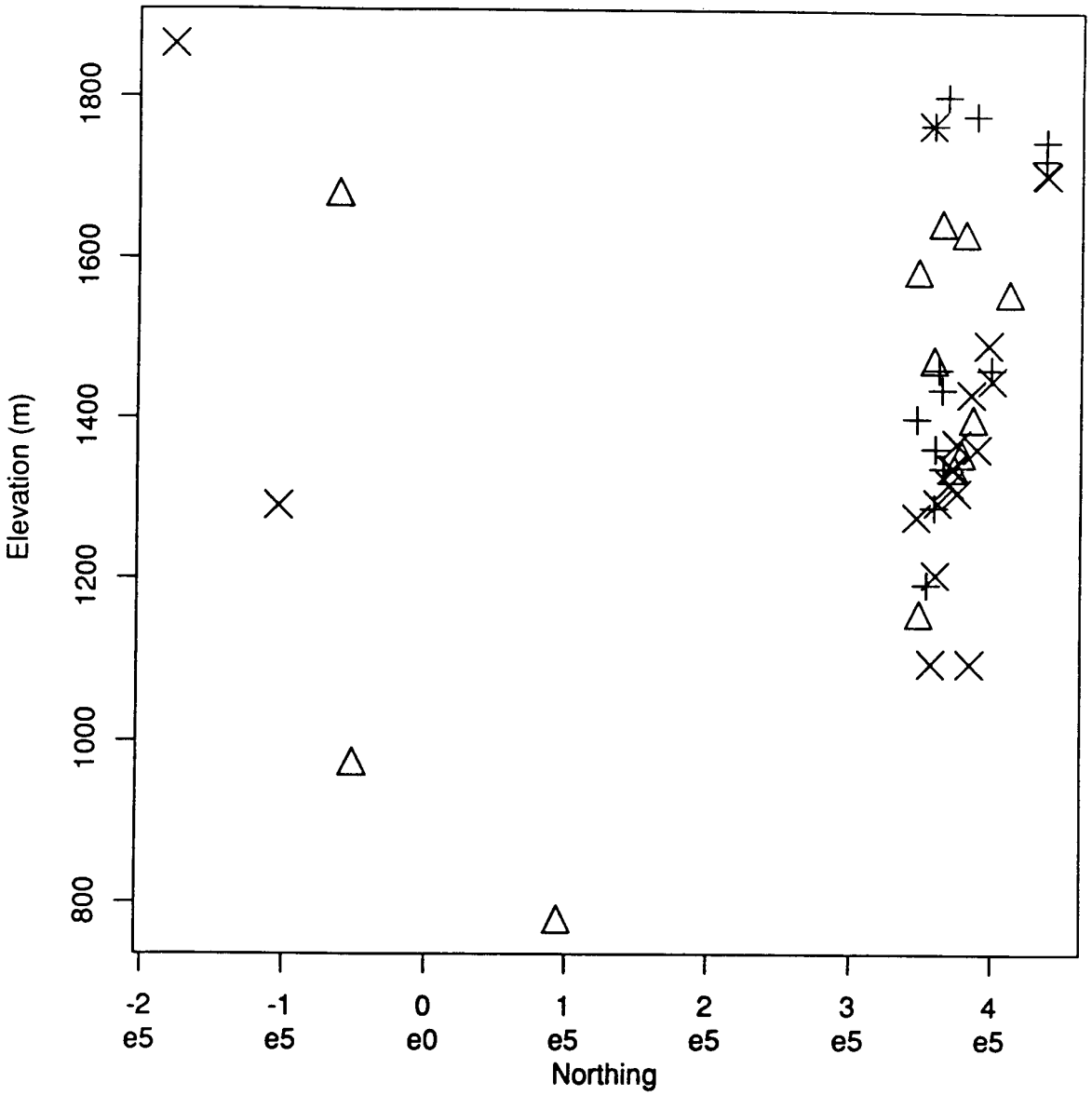

Figure 19. Scatterplot of FIA field plots as a function of latitude and elevation for CALVEG polygons in the Ponderosa Pine type. Symbols for the vegetation types are as follows: triangles - Mixed Conifer/Pine, X - Ponderosa Pine, + - Mixed Conifer/Fir.

3. CONCLUSIONS

Area-class maps provide important spatial information in resource assessments. Because they are simplifications of what in reality is a complex spatial pattern, some degree of inaccuracy is inevitably introduced. The significance of this error depends upon the type of question being asked. That is, the impact of misclassification can be different if one is querying for class at specific sample locations, totaling area by class over the entire map, or investigating change in pattern over time, all of which are typical GIS applications. If all three tasks are to be performed with the same small scale area-class map, careful thought must be given to issues of desired attribute accuracy and spatial resolution.

3.1. Lessons from the analysis of CALVEG

We have distinguished several different kinds of error including errors of polygon misclassification, boundary displacement and over-generalization. Analysis of the CALVEG map indicates that, while all three types of errors are present, misclassification and overgeneralization are much more significant than errors in boundary location produced during map compilation and digitization.

The spatial distribution of errors is of great importance because it affects both the statistical evaluation and the application of the map. Spatial autocorrelation of errors in CALVEG was detected at several scales, including inter-regional differences in error rate, errors for adjacent polygons of closely related vegetation types (e.g., Mixed Conifer/Pine and Mixed Conifer/Fir), and local clustering of errors near boundaries and due to the presence of large inclusions.

Some within polygon heterogeneity is accepted in the process of map generalization (Hole and Campbell 1985). Based on our contingency table analysis, the degree of heterogeneity seems excessive in the CALVEG maps. Two approaches are possible for reducing uncertainty in the map. One approach would be to revise the map by subdividing the existing map units, i.e., increasing spatial resolution, into more homogeneous areas. Alternatively, the map could remain in its original form, but the class definitions could be broadened to account for the variability a user is likely to encounter.

The second pattern of error relates to confusion between taxonomically similar classes, such as was evidenced with the pine and mixed conifer classes. For some purposes, the map could be simplified by moving to a higher level of the classification hierarchy. This would result in fewer classes (less precision) but greater attribute accuracy. Our analysis shows increased accuracy from 42 to 67 percent after class aggregation. In fact, for wildlife habitat analysis in California, this is the approach taken, using just 48 classes (Mayer and Laudenslayer 1988). Clearly, the problems of spatial heterogeneity and taxonomic precision overlap, since related classes may also intersperse in a landscape mosaic or along environmental gradients.

3.2. Future Directions

Within the digital environment now beginning to dominate mapping and inventory work, there is enormous potential for a more appropriate and objective approach to assessing accuracy than has been possible in the past. Despite this, methods remain basically unchanged from pre-digital days. The traditional approach to mapping vegetation cover and assessing timber inventory uses conventional methods of ground check, air photo interpretation and cartography. In rough outline, the land surface is partitioned into areas or "polygons" of greater than a predetermined minimum area, and each area is assigned a land cover class from a standard set of recognized classes. Accuracy is determined both by the geographical scale of mapping, which determines the minimum practical size of the mapping unit, and by the number of available classes. In some cases, codes exist for describing particular "mosaic" categories where two classes am both present in significant amounts. After being transferred to maps, the polygons are digitized and assigned the codes as attributes.

In reality, the earth's surface is not divided into homogeneous areas of greater than some minimum area, by infinitely narrow lines. Areas are heterogeneous to varying degrees, and lines are actually zones of transition of varying width. A cynic once described the process as one of drawing "lines that do not exist around places that have nothing in common". However, as long as a map is assumed to be the desired end product, there are limited avenues for improving the process.

3.2.1. Data collection

Several simple changes in the traditional mapping process would lead to greater sensitivity to data quality, and improvements in estimates of aggregate resources. We recommend that CDF explore the feasibility of these changes in its resource inventory activities:

a) Measures of line quality

The quality of each boundary line should be captured on a simple ordinal scale, such as the following:

1. boundary follows an existing, well-defined feature, e.g. a road
2. boundary follows a clear discontinuity in land cover
3. boundary follows a transition zone or ecotone of less than 20m width
4. boundary follows a transition zone or ecotone of width between 20m and 100m
5. boundary follows a transition zone or ecotone of width greater than 100m.

Although it might be argued that the measures of width in 3, 4 and 5 above be adapted to the scale of mapping, we feel that it would be more useful if they remained constant.

b) Measures of mixtures

We recommend that CDF capture the attributes of each polygon using a coding scheme that recognizes the prevalence of mixtures, and allows the interpreter to code subsidiary as well as the dominant class. Three attribute fields should be assigned to each polygon instead of one, and each should be assigned a percentage rounded to the nearest 10%. Pure stands would be assigned only one attribute, but mixed stands would be assigned two or three. Each attribute field should be assigned sufficient space to code all collected attributes. This approach would recognize the mixed stand as the norm rather than the exception, and allow a more sensitive coding. A similar approach proved successful in the 1:250,000 mapping of California condor habitats (Davis et al. 1989; Stoms et al. 1991).

c) Measures of texture

In conjunction with the above measures, we recommend that CDF initiate procedures for capturing the texture of mixtures. This could be done in one of two ways. First, the interpreter could capture an estimate of mean inclusion size (0 in the case of pure polygons). Altematively, the interpreter could compare each stand to a series of standard pictures of different textures, and identify the most similar. The three measures could be coded as attributes of the AAT, PAT and PAT respectively in ARC/INFO applications.

3.2.2. Sampling

Two alternative sampling strategies are recommended, depending on whether the recommendations above are adopted.

a) Traditional mapping method

The sampling should be stratified by class, to allow for sharply different relative abundances of different classes. Each class should be assigned an equal number of samples. Samples should be taken at points located randomly within the total area of each class (i.e. not stratified by polygon, or located systematically within polygons, or located with respect to access). Locations should be identified using hand-held GPS, to approximately 30m ground accuracy. If a sample point proves to be inaccessible for any reason, it should be replaced by a new randomly sampled point.

The identity or class of the polygon containing each sample point should not be known to the ground crew. The ground crew should not know the location of nearby or containing polygon boundaries.

b) Enhanced mapping method

Samples should be stratified by class as above. However, sample points that would be located in polygons where the dominant class is less than 70% of area should be replaced. Similarly, ground samples should not be taken in polygons where any surrounding arc is of class 4 or higher (i.e. a broad transition zone). Classification should be checked and recorded only for the dominant class in each polygon. Thus sampling should be stratified by the total area in which a given class is dominant.

The purpose of sampling should be to check the identification of classes, not the coding of spatial structure (mixture ratios, texture or boundary quality). If necessary, these measures should be checked by replication, i.e. by having more than one operator map the same area and comparing results.

There are several other questions that CDF needs to consider in revising methods of vegetation mapping and map accuracy assessment:

- how to retrain interpreters in the new concepts;
- what is the per map increase in cost for more accurate data;
- how to represent and store the new information in the database;

- how to generate products such as estimates of area, or overlays on other layers;
- how to present the database information in map form with minimum information loss to the map reader.

Given the strong push to digital spatial databases and GIS, we believe that projects like this will allow CDF to strengthen its reputation for leadership in the development of new methods that take full advantage of the capabilities of GIS and related new technologies.

4. ACKNOWLEDGEMENTS

We grateful for the support and assistance of several individuals. Robin Marose of CDF provided the digital version of the CALVEG map and the FIA sample data, as well as advice and project management. Janine Stenback of CDF provided project management and advice as well as many helpful suggestions on the Draft Final Report. Bob Rogers of the Sequoia National Forest graciously supplied mylars of the timber inventory maps and records of timber inventory plots. A mylar of the 1:250,000 scale CALVEG map for the Bakersfield site was provided by Rich Spradling of the U.S. Forest Service, Pacific Southwest Region. The digital elevation data were obtained from the Map and Imagery Laboratory at the University of California, Santa Barbara. The study was undertaken with the financial support of a Forestry Research Program Grant from the California Department of Forestry and Fire Protection.

REFERENCES

Arbia, G. and R. P. Haining. 1990. Error propagation through map operations, National Center for Geographic Information and Analysis, Santa Barbara.

Blakemore, M.. 1984. Generalization and error in spatial databases. Cartographica 21:131139.

Caceci, M. S. and W. P. Cacheris. May 1984. Fitting curves to data. BYTE 340-360.

Chrisman, N. R.. 1982. Methods of Spatial Analysis Based on Errors on Categorical Maps. Ph.D. Dissertation, Department of Geography, University of Bristol.

Chrisman, N. R. and B. Vandell. 1988. A model for the variance in area. Surveying and Mapping 48:241-246.

Cibula, W. G. and M. 0. Nyquist. 1987. Use of topographic and climatological models in a geographic database to improve Landsat MSS classification for Olympic National Park. Photogrammetric Engineering and Remote Sensing 53:67-75.

Congalton, R. G.. 1988. Using spatial autocorrelation analysis to explore the errors in maps generated from remotely sensed data. Photogrammetric Engineering and Remote Sensing 54:587-592.

Congalton, R. G., R. Oderwald, and R. Mead. 1983. Assessing landsat classification accuracy using discrete multivariate analysis statistical techniques. Photogrammetric Engineering and Remote Sensing 6:169-173.

Davis, F. W., J. Scepan, A Painho, B. Duncan, D. Stoms, and C. Cogan. 1989. Year 2 California Database Project. California Department of Fish and Game Final Report #C2077-2.

Dubayah, R., J. Dozier, and F.W. Davis. 1990. Topographic distribution of clear-sky radiation over the Konza Prairie, Kansas. Water Resources Research 267:679-690.

Duncan, B., M. Painho, and F. Davis. 1990. Utilizing GIS technology for combining regional vegetation maps. Proceedings of GIS/LIS ’90, pp. 1773-1779, Anaheim, California.

Dutton, M.. 1989. Modeling locational. uncertainty via hierarchical tesselation. Pages 125140 in M. F. Goodchild and S. Gopal, editors. Accuracy of Spatial Databases. Taylor and Francis, New York.

Ezcurra, E. and C. Montana. 1984. On the measurement of association between plant species and environmental variables. Acta Oecologica/Oecologia Generalis 5:21-33.

Franklin, W. R.. 1984. Cartographic errors symptomatic of underlying algebra problems. Proceedings, International Symposium on Spatial Data Handling, pp. 190-208, Zurich.

Franklin, W. R. and P. Y. F. Wu. 1987. A polygon overlay system in PROLOG. Proceedings, AutoCarto 8, pp. 97-106, Falls Church, Virginia.

Frolov, Y. S. and D. H. Maling. 1969. The accuracy of area measurements by point counting techniques. Cartographic Journal 6:21-35.

Goodchild, M.. 1980. The effects of generalization in geographical data encoding. Pages 191-205 in H. Freeman and G. Pieroni, editors. Map Data Processing. Academic Press, New York.

Goodchild, M. F.. 1989. Modeling error in objects and fields. Pages 107-114 in M. F. Goodchild and S. Gopal, editors. Accuracy of Spatial Databases. Taylor and Francis, New York.

Goodchild, M. F. and 0. Dubuc. 1987. A model of error for choropleth maps, with applications to geographic information systems. Proceedings, AutoCarto 8, pp. 165-174, ASPRS/ACSM, Falls Church, Virginia.

Goodchild, M. F. and S. Gopal. 1989. Accuracy of Spatial Databases. Taylor and Francis, New York.

Goodchild, M. F. and M. H. Wang. 1988. Modeling error in raster-based spatial data. Proceedings, Third International Symposium on Spatial Data Handling, pp. 97-106, IGU Commission on Geographical Data Sensing and Processing, Sydney.

Greenland, A., R. M. Socher, and M. R. Thompson. 1985. Statistical evaluation of accuracy for digital cartographic data bases. Proceedings, AutoCarto 7, pp. 212-221, ASPRS/ACSM, Falls Church, Virginia.

Griffith, D. A.. 1989. Distance calculations and errors in geographic databases. Pages 81-90 in M. F. Goodchild and S. Gopal, editors. Accuracy of Spatial Databases. Taylor and Francis, New York.

Heuvelink, G.B.M., P.A. Burrough, and A. Stein. 1989. Propagation of errors in spatial modelling with GIS. Int. J. Geographical Information Systems 3:303-322.

Hoffer, R. M., M. D. Fleming, L. A. Bartolucci, S. M. Davis, and R. F. Nelson. 1979. Digital processing of Landsat MSS and topographic data to improve capabilities for computerized mapping of forest cover types. LARS Technical Report 011579:159.

Holdridge, L.R., W. C. Grenke, W. H. Hathaway, T. Liang, and J. A. Tosi. 1971. Forest Environments in Tropical Life Zones: A Pilot Study. Pergamon, Oxford.

Hole, F. D. and J. B. Campbell. 1985. Soil landscape analysis. Rowan and Allanheld, Totowa, New Jersey.

Keefer, B. J., J. L. Smith, and T. G. Gregoire. 1988. Simulating manual digitizing error with statistical models. Proceedings, GIS/LIS '88, pp. 475-83, ASPRS/ACSM, Falls Church, Virginia .

Kuchler, A. W.. 1977. A Map of the Natural Vegetation of California. Pages 909-938 in M. G. Barbour and J. Major, editors. TerTestrial Vegetation of California. John Wiley and Sons, New York.

Lodwick, W. A.. 1989. Developing confidence limits on errors of suitability analyses in geographical information systems. Pages 69-78 in M. F. Goodchild and S. Gopal, editors. Accuracy of Spatial Databases. Taylor and Francis, New York.

Lodwick, W. A. and W. Monson. 1988. Sensitivity analysis in geographic information systems. Department of Mathematics Paper RP886, University of Colorado, Denver.

Mark, D. M. and F. Csillag. 1989. The nature of boundaries on area- class maps. Cartographica 21:65-78.

Matayas, W. J. and I. Parker. 1980. CALVEG: A Classification of Californian Vegetation, Regional Ecology Group, U. S. Forest Service, San Francisco.

Mayer, K. E. and W. F. Laudenslayer. 1988. A guide to the wildlife habitats of California. Regional Ecology Group, California Department of Forestry aand Fire Protection, Sacramento, California.

McKay, N.. 1987. How the statewide hardwood assessment was conducted. Pages 298-303 in T. R. Plumb and N. H. Pillsbury, editors. Proceedings of the Symposium on Multipleuse Management of California's Hardwood Resources. United States Forest Service Pacific Southwest Forest and Range Experiment Station.

Mead, R. A. and J. Szajgin. 1982. Landsat classification accuracy assessment procedures. Photogrammetric Engineering and Remote Sensing 48:139-141.

Newcomer, J. A. and J. Szajgin. 1984. Accumulation of thematic map errors in digital overlay analysis. The American Cartographer 11:58-62.

Oliver, A.0. and R. Webster. 1986. Semi-variograms for modelling the spatial pattern of landform and soil properties. Earth Surface Processess and Landforms 11:491-504.

Perkal, J.. 1956. On epsilon length. Bulletin de I'Academie Polonaise des Sciences 4:399403.

Perkal, J.. 1966. On the length of empirical curves. Discussion Paper No. 10, Michigan Inter-University Community of Mathematical Geographers, Ann Arbor.

Rosenfield, G. H.. 1986. Analysis of thematic map classification err-or matrices. Photogrammetric Engineering and Remote Sensing 52:681-686.

Rosenfield, G. H. and K. Fitzpatrick-Lins. 1986. A coefficient of agreement as a measure of thematic map accuracy. Photogrammetric Engineering and Remote Sensing 52:223-227.

Rosenfield, G. H.. 1986. Analysis of thematic map classification error matrices. Photogrammetric Engineering and Remote Sensing 52:681-686.

Rosenfield, G. H. and K. Fitzpatrick-Lins. 1986. A coefficient of agreement as a measure of thematic map accuracy. Photogrammetric Engineering and Remote Sensing 52:223-227.

Stoms, D. M., F. W. Davis, and C. B. Cogan. 1991. Sensitivity of wildlife habitat models to uncertainties in GIS data. Photogrammetric Engineering and Remote Sensing,ln press.

Strahler, A.H.. 1981. Stratification of natural vegetation for forest and rangeland inventory using Landsat digital imagery and collateral data. International Journal of Remote Sensing 2:15-41.

Tosta, N. and R. Marose. 1987. The Distribution of California Hardwoods: Results of a Statewide Geographic Information System. Pages 304-308 in T. R. Plumb and N. H. Pillsbury, editors. Proceedings of the Symposium on Multiple-Use Management of California's Hardwood Resources. Pacific Southwest Forest and Range Experiment Station, San Luis Obispo.

Vankat, J. L.. 1982. A gradient perspective on the vegetation of Sequoia National Park, California. Madroo 29:200-214.

Van Genderen, J. L. and B. F. Lock. 1977. Testing land-use map accuracy. Photogrammetric Engineering and Remote Sensing 43:1135-1137.

Van Genderen, J. L., B. F. Lock, and P. A. Vass. 1978. Remote sensing: statistical testing of thematic map accuracy. Remote Sensing of Environment 7:3-14.

Veregin, H.. 1989. Error modeling for the map overlay operation. Pages 3-18 in M. F. Goodchild and S. Gopal, editors. Accuracy of Spatial Databases. Taylor and Francis, New York.

Yool, S. R., J. L. Star, J. E. Estes, D. B. Botkin, D. W. Eckhardt, and F. W. Davis. 1986. Performance analysis of image processing algorithms for classification of natural vegetation in the mountains of southern California. International Journal of Remote Sensing 7:683-702.